

Table 1. Top Single Nucleotide Polymorphisms Based on GWAS and Meta-Analysis

CHR	SNP	BP	Closest Gene	Meta_ALL (JPN_GWAS+Rep_JPN+UK_SCZ)				Meta_JPN (JPN_GWAS+Rep_JPN)				JPN_GWAS		Rep_JPN		UK_SCZ				
				A1	MAF	A2	P _{CMH}	OR ^a	L95	U95	P _{CMH}	OR ^a	L95	U95	P _{allele}	OR ^a	P _{allele}	OR ^a	P _{allele}	OR ^a
2	rs11895771	37266439	SULT6B1	T	.49	G	3.7×10^{-5}	.84	.77	.91	4.1×10^{-4}	.84	.76	.92	8.0×10^{-6}	.64	.14	.92	.033	.84
7	rs1011131	19474460	LOC392288	G	.07	C	1.2×10^{-4}	1.30	1.14	1.48	1.2×10^{-4}	1.31	1.14	1.50	2.5×10^{-5}	1.78	.054	1.17	.63	1.14
14	rs1176970	40505514	LOC644919	G	.15	C	1.4×10^{-4}	1.22	1.10	1.35	3.0×10^{-4}	1.27	1.12	1.44	3.2×10^{-4}	1.58	.041	1.17	.14	1.14
1	rs4908274	103162502	COL11A1	A	.28	T	3.1×10^{-4}	1.20	1.09	1.32	3.1×10^{-4}	1.20	1.09	1.32	1.1×10^{-4}	1.45	.067	1.12	NA	NA
6	rs2294424	11860537	C6orf105	T	.41	C	5.0×10^{-4}	1.15	1.06	1.24	5.0×10^{-4}	1.17	1.28	1.07	1.2×10^{-4}	1.40	.081	1.1	.41	1.08
2	rs13010889	40617519		A	.15	C	.0011	.85	.77	.94	.0016	.85	.77	.94	8.7×10^{-5}	.67	.17	.92	.40	.84
2	rs17026152	40611159		A	.26	G	.0012	.85	.77	.94	.0012	.85	.77	.94	1.3×10^{-4}	.69	.15	.92	NA	NA
6	rs2787566	101985455	GRIK2	A	.04	G	.0014	1.34	1.12	1.61	.0014	1.39	1.1	1.7	2.8×10^{-4}	2.03	.15	1.19	.49	1.16
6	rs2071286	32287874	NOTCH4	T	.19	C	.0014 ^b	.87	.79	.95	.0049 ^b	.86	.78	.96	3.3×10^{-4}	.68	.23 ^b	.93	.13	.87
8	rs17462248	29426926		G	.2	T	.0017	1.16	1.06	1.27	.020	1.14	1.0	1.3	2.1×10^{-4}	1.52	.60	1.04	.030	1.2

p values were calculated on the basis of the allele-wise test (two-tailed).

A1, minor allele based on whole sample; A2, major allele based on whole sample; BP, base position; CHR, chromosome(hg18); GWAS, genome-wide association study; JPN_GWAS, our screening GWAS; L95, lower bound of 95% confidence interval for OR; MAF, minor allele frequency based on whole sample; NA, not analyzed; OR, odds ratio; SNP, single nucleotide polymorphism; U95, upper bound of 95% confidence interval for odds ratio, UK-SCZ: UK schizophrenia.

^aOR was calculated on the basis of A1 in Meta-ALL as reference.

^bControls from Japanese SNPs (JSNP) were merged into the replication sample.

data set because of the high missing rate of 12%). Next we conducted a meta-analysis based on Meta_JPN (imputed data from JPN_GWAS was down-weighted using PROPER-INFO from SNPTEST by METAL: <http://www.sph.umich.edu/csg/abecasis/metal/>) and the sample of Tochigi (18). This provided fairly strong evidence for association ($P_{meta} = 5.1 \times 10^{-5}$, two-tailed, Figure S5 in Supplement 1).

Polygenic Component Analysis

p values and pseudo-*R*² statistics (Nagaelkerke's *R*²) for the analysis based on the split Japanese sample are presented in Figure 1 and in Table S3 in Supplement 1. The polygenic scores in the target data were higher in the cases than the controls and, in most cases, significantly so. As in the ISC study, the evidence became stronger and the pseudo-*R*² improved at more liberal *P*_T values. The most significant correlation was found at *P*_T < .5 (*p* = .005). In this condition, the pseudo-*R*² was slightly lower (*R*² = .021) compared with the ISC study (6) in which *R*² ≤ .032 were observed in the Caucasian samples (Figure 1), although we note that the ISC study used information from a greater number of SNPs, with the larger sample available to that group allowing the inclusion of SNPs with MAF as low as 2%.

The results of the analysis based on discovery in the UK schizophrenia data set and targeting the JPN_GWAS are shown in Figure 2 (Table S3 in Supplement 1). Again, as with the ISC data, the signal and predictive power improved at the more liberal thresholds, with only the most relaxed threshold (corresponding to the optimal threshold from the ISC study) attaining significance (*p* = .029). However, the analysis using the WTCCC bipolar sample for discovery and the Japanese as the target did not reveal significant support for shared risk across disorders (Figure 2 and Table S3 in Supplement 1).

Following are the results of the analyses based on discovery in the JPN_GWAS and testing in the UK schizophrenia and bipolar data sets. Alleles trained in this direction were highly significant, but weakly predictive, of schizophrenia status in the UK sample (*p*_{min} = 7.0×10^{-5}) than those analyses based on training in the UK data sets. Again, no significant effect was observed for bipolar disorder. In the schizophrenia analysis, we observed no clear relationship

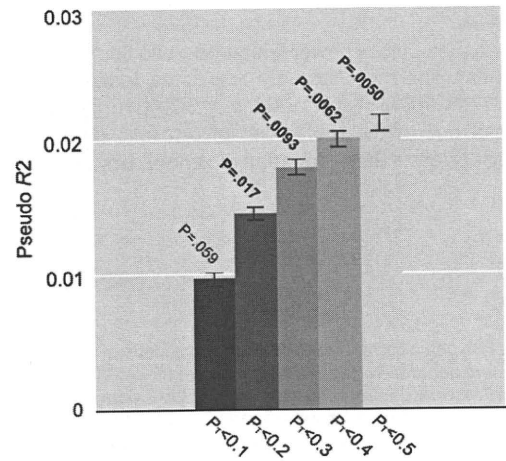


Figure 1. Polygenic component analysis for the pair within screening genome-wide association studies samples. *p*_T = *p* threshold. Pseudo *R*² and *p* values represent the mean and median values, respectively, from 1000 random divisions of the data set. Error bars represent the 95% confidence intervals for *R*² from those repeat analyses. Bold numbers represent significant *p* values (< .05).

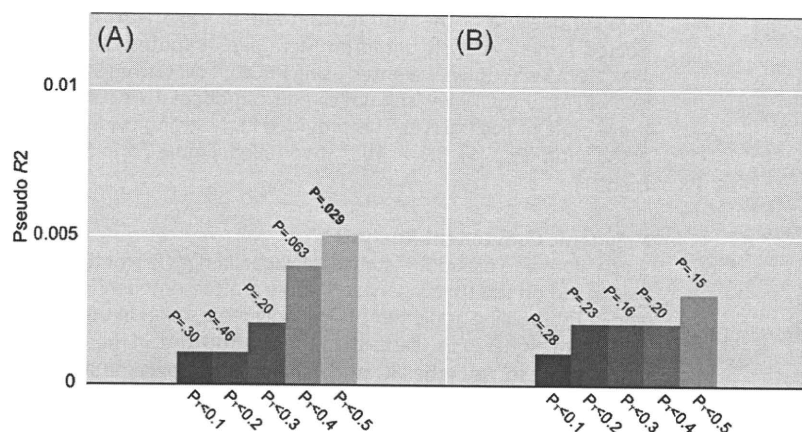


Figure 2. Polygenic component analysis for the pairs of Wellcome Trust Case-Control Consortium (WTCCC) data sets/screening genome-wide association studies (GWAS). (A) UK schizophrenia/screening GWAS discovery/target pair. (B) WTCCC bipolar/screening GWAS discovery/target pair. $p_T = p$ threshold. Bold numbers represent significant p values ($< .05$).

between the test allele significance threshold (p_T) and either the statistical support or the pseudo- R^2 (Figure 3 and Table S3 in Supplement 1).

Discussion

In this study, we did not detect unequivocal evidence for a novel susceptibility gene for schizophrenia, although our results do provide weak support for association between *SULT6B1* and schizophrenia, and our analyses of previously implicated regions and candidate genes provide support for the hypothesis that previous findings at the MHC region of chromosome 6 may point to *NOTCH4*. The absence of association at genome-wide levels of significance is not surprising given the relatively small size of our GWAS. Recent large-scale GWAS of schizophrenia suggest that the effect sizes of common risk alleles are small (ORs < 1.25). Power analysis suggests that our GWAS has only .18% power under an additive model to detect at $\alpha = 7.2 \times 10^{-8}$, a susceptibility variant with an allele frequency of .3 conferring an OR of 1.25. Clearly, with power like this, it would be extremely unlikely that any one locus would be detected at strong levels of support; however, in the presence of a thousand or more loci as has been suggested (6), the power to detect at least one of these would be considerably greater, albeit the subsequent power to replicate that specific locus would once again be low.

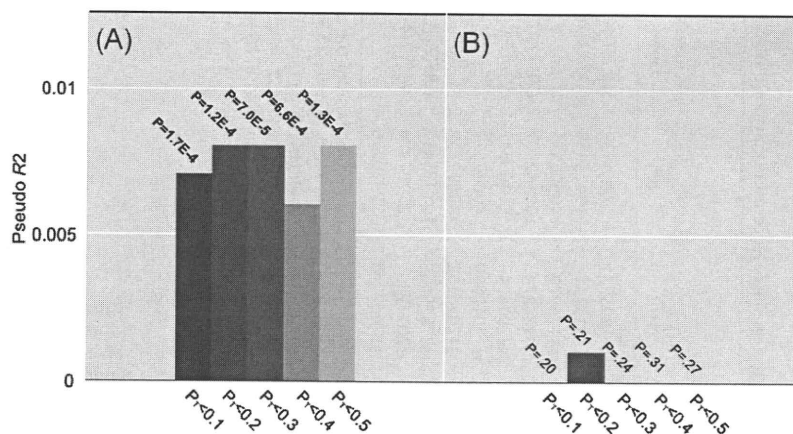
Despite the obvious power limitations, two findings are worthy of comment. The most strongly associated individual SNP was rs11895771 at *SULT6B1* (Meta-ALL $p = 3.7 \times 10^{-5}$). *SULT6B1* is a member of one of the subfamilies of cytosolic sulfotransferases (SULT) that catalyze the sulfonation of xenobiotics, hormones, and

neurotransmitters, including 17β -estradiol and corticosterone (19), functions that are at least plausibly related to schizophrenia (20–22), and brain function (23–25) more widely.

The second locus of interest was *NOTCH4*. *NOTCH4* has been reported to be associated with schizophrenia in a small UK sample (26) (not overlapping with the present sample), but replication data from candidate gene studies have not been strongly supportive. However, a recent synthesis of GWASs as well as a large number of additional subjects reported a genome-wide significant association at rs3131296 (8), which is located within *NOTCH4* (Figure S2 in Supplement 1), although the extensive LD across the MHC region makes pinpointing the source of that signal to a specific gene impossible. It is therefore of interest in our evaluation of the MHC region that the signal clearly maximized to the *NOTCH4* region (Figure S2 in Supplement 1), lending support to the hypothesis that this may be the relevant susceptibility gene in the region. We are unable to evaluate the specific SNP (rs3131296) reported in the SGENE study for the Japanese population because of the failure of imputation. In the Japanese population, the MAF of rs3131296 differs considerably from that in Europeans (MAF = 10% and 2.3% for CEU and JPT populations, respectively, in HapMap Phase 3 data, 13% reported in SGENE), which means the ability of this marker to tag a common functional variant is likely to differ significantly between populations. Given the evidence for association observed in our study and the prior genetic evidence for *NOTCH4*, this locus warrants further detailed analysis in larger and more ethnically diverse samples.

This study provides the first independent (of the samples used by the ISC) replication of the polygenic score analysis reported by

Figure 3. Polygenic component analysis for the pairs of the screening genome-wide association studies (GWAS)/Wellcome Trust Case-Control Consortium (WTCCC) data sets. (A) Screening GWAS/UK schizophrenia discovery/target pair. (B) Screening GWAS/WTCCC bipolar discovery/target pair. $p_T = p$ threshold. Bold numbers represent significant p values ($< .05$).



the ISC (6). Although our sample is low powered (power is .6 for our full sample and .56 for half of the sample to detect at an alpha level of .5, a weak genetic effect [OR 1.1] conferred by an allele with a frequency of .3), the set of “risk” alleles (in quotation marks to emphasize that most are not likely to be true risk alleles) derived from half of the Japanese sample was significantly correlated with affection status in the other half of the samples. One possible important confounding factor to consider is an effect of population stratification. To check for this as a possible effect, we used 1) principal components analysis–adjusted (the first 10 principal components) discovery statistics for the selection of SNPs and 2) the first 10 principal component vectors as covariates in calculating the polygenic score in the target sample. However, the application of either or both of these did not lead to a material difference in the results (Table S4 in Supplement 1), indicating that stratification is not likely to explain our replication of the ISC findings.

Our Japan–UK analyses also suggests this effect is unlikely to be due to stratification (this was also convincingly argued in the ISC study) because the Japanese and UK schizophrenia samples are ascertained directionally for the same stratification biases and because the UK schizophrenia sample, but not the UK bipolar sample, would be unlikely to be stratified in that manner. Instead, those data point to a shared genetic component to schizophrenia susceptibility across major ethnic groups, as predicted by an effect driven by common “risk” alleles rather than rare alleles, although not excluding an effect of rare alleles, which are much more likely to reside on different haplotype backgrounds in different populations. However, there is also evidence for population differences in risk. Thus, the analyses restricted to the Japanese population showed much higher maximal estimates for R^2 (.021) compared with the analyses of schizophrenia between populations ($R^2 = .005 \sim .008$) and was more similar to the estimates of R^2 when the analyses were performed within European populations (6). The ISC also undertook one cross-population analysis, between Caucasian and African Americans. As in our study, R^2 was much lower between the ethnic groups (.004) than within the European populations. These results suggest that although at least some “risk” alleles are shared across populations, there are also differences in those “risk” alleles or at least in the extent to which they are tagged by markers at the density currently provided by the arrays we have studied. At a practical level, this means that failures to replicate findings across ethnic groups, even with respect to common alleles, should be treated with considerable caution.

One intriguing finding was our failure to find evidence that “risk” alleles for bipolar disorder in the European sample predict risk of schizophrenia in the Japanese sample (or vice versa). One likely explanation is that there is only a partial overlap between “risk” alleles for schizophrenia and bipolar disorder and that this, together with the additionally reduced R^2 because of ethnic differences, has affected our ability to demonstrate an effect. This interpretation is at least partially consistent with the ISC study in which the measures of R^2 that were observed in bipolar data sets were less than those observed in the schizophrenia data sets. A more interesting but speculative interpretation is that the Japanese sample represents a phenotypically purer form of schizophrenia than the European samples. These hypotheses require further evaluation in larger Japanese samples, exploration of aspects of the schizophrenia phenotype in the European samples, and transdiagnostic polygenic score analyses within Japanese samples.

This work was supported in part by research grants from the Japan Ministry of Education, Culture, Sports, Science and Technology; the Ministry of Health, Labor and Welfare; the Core Research for Evolu-

tional Science and Technology; and the Health Sciences Foundation (Research on Health Sciences focusing on Drug Innovation). The UK research was supported by grants from the Medical Research Council and the Wellcome Trust.

The authors MCO and NI are joint last authors.

Dr. Ikeda reports receiving support from the Japan Society for the Promotion of Science postdoctoral fellowship for research abroad and is also supported by the Uehara Memorial Foundation and the Great Britain Sasakawa Foundation. The other authors report no biomedical financial interests or potential conflicts of interest.

Supplementary material cited in this article is available online.

- O'Donovan MC, Craddock NJ, Owen MJ (2009): Genetics of psychosis: insights from views across the genome. *Hum Genet* 126:3–12.
- O'Donovan MC, Craddock N, Norton N, Williams H, Peirce T, Moskva V, *et al.* (2008): Identification of loci associated with schizophrenia by genome-wide association and follow-up. *Nat Genet* 40:1053–1055.
- Steinberg S, Mors O, Borglum AD, Gustafsson O, Werge T, Mortensen PB, *et al.* (2010): Expanding the range of ZNF804A variants conferring risk of psychosis [published online ahead of print January 5]. *Mol Psychiatry*.
- Riley B, Thiselton D, Maher BS, Bigdeli T, Wormley B, McMichael GO, *et al.* (2010): Replication of association between schizophrenia and ZNF804A in the Irish Case–Control Study of Schizophrenia sample. *Mol Psychiatry* 15:29–37.
- Williams HJ, Norton N, Dwyer S, Moskva V, Nikolov I, Carroll L, *et al.* (2010): Fine mapping of ZNF804A and genome-wide significant evidence for its involvement in schizophrenia and bipolar disorder [published online ahead of print April 6].
- International Schizophrenia Consortium, Purcell SM, Wray NR, Stone JL, Visscher PM, O'Donovan MC, *et al.* (2009): Common polygenic variation contributes to risk of schizophrenia and bipolar disorder. *Nature* 460:748–752.
- Shi J, Levinson DF, Duan J, Sanders AR, Zheng Y, Pe'er I, *et al.* (2009): Common variants on chromosome 6p22.1 are associated with schizophrenia. *Nature* 460:753–757.
- Stefansson H, Ophoff RA, Steinberg S, Andreassen OA, Cichon S, Rujescu D, *et al.* (2009): Common variants conferring risk of schizophrenia. *Nature* 460:744–747.
- Wray NR, Visscher PM (2009): Narrowing the boundaries of the genetic architecture of schizophrenia. *Schizophr Bull* 36:14–23.
- Evans DM, Visscher PM, Wray NR (2009): Harnessing the information contained within genome-wide association studies to improve individual prediction of complex disease risk. *Hum Mol Genet* 18:3525–3531.
- Craddock N, O'Donovan MC, Owen MJ (2009): Psychosis genetics: Modeling the relationship between schizophrenia, bipolar disorder, and mixed (or “schizoaffective”) psychoses. *Schizophr Bull* 35:482–490.
- Craddock N, O'Donovan MC, Owen MJ (2007): Symptom dimensions and the Kraepelinian dichotomy. *Br J Psychiatry* 190:361; author reply: 361–362.
- Yamaguchi-Kabata Y, Nakazono K, Takahashi A, Saito S, Hosono N, Kubo M, *et al.* (2008): Japanese population structure, based on SNP genotypes from 7003 individuals compared to other ethnic groups: Effects on population-based association studies. *Am J Hum Genet* 83:445–456.
- Wellcome Trust Case-Control Consortium (2007): Genome-wide association study of 14,000 cases of seven common diseases and 3,000 shared controls. *Nature* 447:661–678.
- Ikeda M, Aleksic B, Kirov G, Kinoshita Y, Yamanouchi Y, Kitajima T, *et al.* (2009): Copy number variation in schizophrenia in the Japanese population. *Biol Psychiatry* 67:283–286.
- Purcell S, Neale B, Todd-Brown K, Thomas L, Ferreira MA, Bender D, *et al.* (2007): PLINK: A tool set for whole-genome association and population-based linkage analyses. *Am J Hum Genet* 81:559–575.
- Dudbridge F, Gusnanto A (2008): Estimation of significance thresholds for genomewide association scans. *Genet Epidemiol* 32:227–234.
- Tochigi M, Zhang X, Ohashi J, Hibino H, Otowa T, Rogers M, *et al.* (2007): Association study between the TNXB locus and schizophrenia in a Japanese population. *Am J Med Genet B Neuropsychiatr Genet* 144B:305–309.

19. Cao H, Agarwal SK, Burnside J (1999): Cloning and expression of a novel chicken sulfotransferase cDNA regulated by GH. *J Endocrinol* 160:491–500.
20. Eaton WW, Byrne M, Ewald H, Mors O, Chen CY, Agerbo E, Mortensen PB (2006): Association of schizophrenia and autoimmune diseases: Linkage of Danish national registers. *Am J Psychiatry* 163:521–528.
21. Baumgartner A, Pietzcker A, Gaebel W (2000): The hypothalamic-pituitary-thyroid axis in patients with schizophrenia. *Schizophr Res* 44:233–243.
22. Kulkarni J, de Castella A, Fitzgerald PB, Gurvich CT, Bailey M, Bartholomeusz C, Burger H (2008): Estrogen in severe mental illness: A potential new treatment approach. *Arch Gen Psychiatry* 65:955–960.
23. Cerqueira JJ, Pego JM, Taipa R, Bessa JM, Almeida OF, Sousa N (2005): Morphological correlates of corticosteroid-induced changes in prefrontal cortex-dependent behaviors. *J Neurosci* 25:7792–7800.
24. Enkel T, Koch M (2009): Chronic corticosterone treatment impairs trace conditioning in rats with a neonatal medial prefrontal cortex lesion. *Behav Brain Res* 203:173–179.
25. Gogos A, Nathan PJ, Guille V, Croft RJ, van den Buuse M (2006): Estrogen prevents 5-HT1A receptor-induced disruptions of prepulse inhibition in healthy women. *Neuropsychopharmacology* 31:885–889.
26. Wei J, Hemmings GP (2000): The NOTCH4 locus is associated with susceptibility to schizophrenia. *Nat Genet* 25:376–377.

Phenotypic Characterization of Transgenic Mice Overexpressing Neuregulin-1

Taisuke Kato¹, Atsushi Kasai², Makoto Mizuno^{1,3}, Liang Fengyi⁴, Norihito Shintani⁵, Sadaaki Maeda², Minesuke Yokoyama⁶, Miwako Ozaki^{7,8}, Hiroyuki Nawa^{1,3*}

1 Department of Molecular Neurobiology, Brain Research Institute, Niigata University, Niigata, Japan, **2** Department of Pharmacotherapeutics, Faculty of Pharmaceutical Sciences, Setsunan University, Osaka, Japan, **3** Center for Transdisciplinary Research, Niigata University, Niigata, Japan, **4** Department of Anatomy, Yong Loo Lin School of Medicine, National University of Singapore, Singapore, Singapore, **5** Department of Molecular Neuropharmacology, Graduate School of Pharmaceutical Sciences, Osaka University, Suita, Osaka, Japan, **6** Center for Bioresource-Based Researches, Brain Research Institute, Niigata University, Niigata, Japan, **7** Consolidated Research Institute for Advanced Science and Medical Care, Waseda University, Tokyo, Japan, **8** Neuroscience and Neuroengineering Group, Waseda Bioscience Institute of Singapore (WABIOS), Helios, Singapore

Abstract

Background: Neuregulin-1 (NRG1) is one of the susceptibility genes for schizophrenia and implicated in the neurotrophic regulation of GABAergic and dopaminergic neurons, myelination, and NMDA receptor function. Postmortem studies often indicate a pathologic association of increased NRG1 expression or signaling with this illness. However, the psychobehavioral implication of NRG1 signaling has mainly been investigated using hypomorphic mutant mice for individual NRG1 splice variants.

Methodology/Principal Findings: To assess the behavioral impact of hyper NRG1 signaling, we generated and analyzed two independent mouse transgenic (Tg) lines carrying the transgene of green fluorescent protein (GFP)-tagged type-1 NRG1 cDNA. The promoter of elongation-factor 1 α gene drove ubiquitous expression of GFP-tagged NRG1 in the whole brain. As compared to control littermates, both heterozygous NRG1-Tg lines showed increased locomotor activity, a nonsignificant trend toward decreasing prepulse inhibition, and decreased context-dependent fear learning but exhibited normal levels of tone-dependent learning. In addition, social interaction scores in both Tg lines were reduced in an isolation-induced resident-intruder test. There were also phenotypic increases in a GABAergic marker (parvalbumin) as well as in myelination markers (myelin basic protein and 2',3'-cyclic nucleotide 3'-phosphodiesterase) in their frontal cortex, indicating the authenticity of NRG1 hyper-signaling, although there were marked decreases in tyrosine hydroxylase levels and dopamine content in the hippocampus.

Conclusions: These findings suggest that aberrant hyper-signals of NRG1 also disrupt various cognitive and behavioral processes. Thus, neuropathological implication of hyper NRG1 signaling in psychiatric diseases should be evaluated with further experimentation.

Citation: Kato T, Kasai A, Mizuno M, Fengyi L, Shintani N, et al. (2010) Phenotypic Characterization of Transgenic Mice Overexpressing Neuregulin-1. *PLoS ONE* 5(12): e14185. doi:10.1371/journal.pone.0014185

Editor: Thomas Burne, University of Queensland, Australia

Received: January 22, 2010; **Accepted:** November 10, 2010; **Published:** December 9, 2010

Copyright: © 2010 Kato et al. This is an open-access article distributed under the terms of the Creative Commons Attribution License, which permits unrestricted use, distribution, and reproduction in any medium, provided the original author and source are credited.

Funding: This work was supported by Health and Labor Sciences Research Grants, a grant for Promotion of Niigata University Research Projects, Core Research for Evolutional Science and Technology from the Japan Science and Technology Agency, and a grant-in-aid from the Ministry of Health, Labour and Welfare of Japan. Hiroyuki Nawa was a recipient of research grants from AstraZeneca Pharmaceutical. No funders had a role in either the study design, data collection and analysis, decision to publish, or preparation of the manuscript.

Competing Interests: HN was a recipient of the research grants from AstraZeneca Pharmaceutical, Inc. This does not alter the authors' adherence to the PLoS ONE policies on sharing data and materials.

* E-mail: hnawa@bri.niigata-u.ac.jp

Introduction

A genetic association between the neuregulin-1 (NRG1) gene and schizophrenia has been documented in various human populations. However, the exact biological relationship is still unclear [1–3]. Many model studies have used NRG1 hypomorphic mutant mice to study the phenotypic consequences of decreased NRG1 signaling as well as its pathologic contribution to schizophrenia [2], [4–13]. Differential promoter usage and alternative splicing produce a large variety of structural variants of NRG1 precursor proteins. For example, the type-1, -2, and -4 subgroups of NRG1 contain a immunoglobulin-like domain

and a transmembrane domain while the type-3 variant carries two transmembrane domains and a cystein-rich domain [14], [15]. Mutant mice deficient in NRG1 have been found to exhibit schizophrenia-associated behavioral abnormalities in sensorimotor gating [2], [4], social interactions [5], [9–11], latent inhibition [12], and locomotor activity [8], [13], although neurobehavioral features of the individual mutants significantly differ depending upon the targeted isoforms of NRG1 [2], [6], [7–13]. NRG1 has neurotrophic activities to promote NMDA receptor expression, GABA synthesis, and myelination, all of which are diminished in postmortem brain of schizophrenia patients [14], [15]. The animal and patient studies suggest that

decreased NRG1 signals are responsible for the pathophysiology of schizophrenia [14], [15]. However, this argument is not supported by all types of studies. For example, postmortem studies report that higher levels of type-1 and type-4 NRG1 mRNA are present in the hippocampus and prefrontal cortex of schizophrenic patients as well as in patients' lymphocytes, compared to control subjects [16–19]. Similarly, the up-regulation of the NRG1 protein or its signaling is detected in the brains of schizophrenic patients [20], [21]. Thus, these patient studies rather suggest a biological link between increased NRG1 signaling and the pathophysiology of schizophrenia. As the type-1 NRG1 variant display marked mRNA increase in patients' postmortem brain and single nucleotide polymorphisms (SNPs) of its corresponding genome locus are implicated in genetic vulnerability to schizophrenia [18], [19], we have established mouse transgenic lines carrying the transgene of mouse type-1 NRG1 cDNA and examined whether NRG1 hypermorphic mice, as opposed to NRG1 hypomorphic mice, are an appropriate animal model for schizophrenia. In the present investigation, we analyzed two independent transgenic (Tg) mouse lines to minimize the effects of the transgene insertion in their host genome as well as those of the genetic inhomogeneity of mouse genetic background. Further, we examined neurochemical consequences of NRG1 overexpression in several neuronal and glial markers in one of the Tg lines. Behavioral similarity and difference between the present Tg mice and reported NRG1-knockout mice are also discussed.

Results

Generation of transgenic mice overexpressing NRG1

We constructed the Tg vector that contained the promoter of a house keeping gene, elongation-factor 1 α (EF1 α) and GFP-tagged NRG1 β 1 cDNA. The GFP-tag facilitated transgene expression and detection in mice. The Tg vector was injected to fertilized eggs to generate transgenic mice (Fig. 1A). The modification of GFP tagging is known not to affect NRG1 function [22]. We selected two independent NRG1-Tg lines, Tg5 and Tg7, which were viable and healthy with normal body weights and reproduction (data not shown). The number of transgene copies integrated in genome was estimated by polymerase chain reaction (PCR). Densitometric measurement revealed that PCR products from Tg5 DNA first appeared at ~22 cycle and that from Tg7 at ~24 cycle, 3–4 and 1–2 cycle earlier than the emergence of wild type (WT) mice product (2 copies of wild allele) respectively (Fig. 1B). Based on the present efficiency of PCR amplification (1.6 \pm 0.1 fold/cycle), we estimated that Tg5 mouse contained 5–6 copies of the transgene and Tg7 mouse carried ~2 copies. To confirm the expression of the transgene in the brain, we performed an immunoblotting analysis with anti-NRG1 and anti-GFP antibodies. There were NRG1-like and GFP-like immunoreactivities at the same size (55 kDa) in whole brain lysates of Tg5 and Tg7 (Fig. 1C). The size approximately matches the sum of molecular weights of GFP (25 kDa) and a shedded mature form of NRG1 β 1 (30 kDa). The Tg5 line contained higher levels of

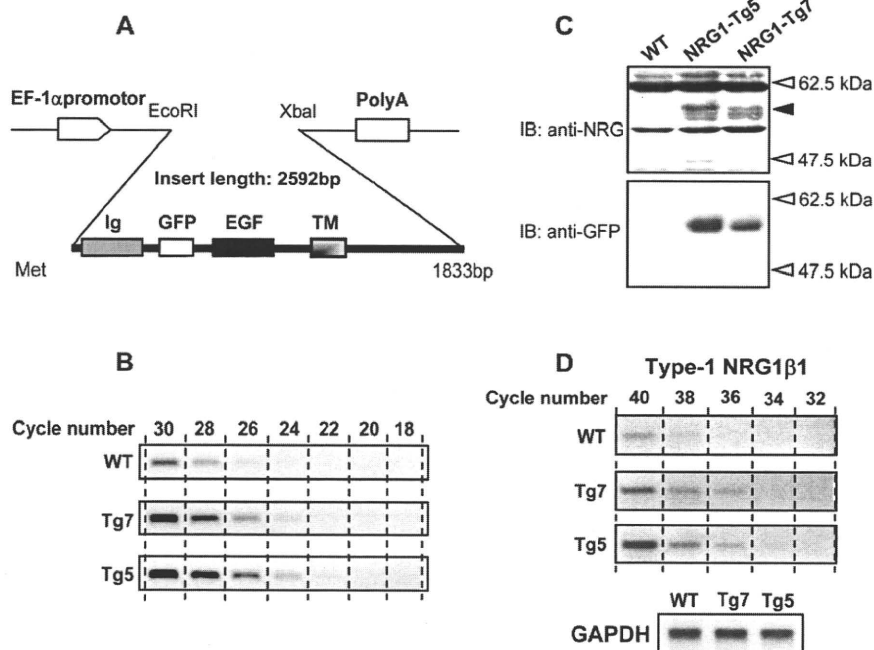


Figure 1. Establishment of GFP-tagged NRG1 transgenic mice with EF1 α -promoter. (A) A schematic illustration of a transgene construct carrying EF-1 α genomic promoter, NRG1 β 1 cDNA, GFP-tag insertion, and poly A signal. (B) Estimation of the copy number of the transgene by PCR. The exon 3 fragment of NRG1 genome was amplified with 18–30 cycles using tail DNA from Tg5 and Tg7 and separated in an agarose-gel. (C) Protein lysate was prepared from whole brain of adult male NRG1-Tg mice (Tg5 and Tg7) and WT littermate and subjected to immunoblotting with anti-NRG1 and anti-GFP antibodies. A closed arrowhead marks the transgene products. (D) Quantification of mRNA levels for type-1 NRG1 by RT-PCR. cDNA fragments specific for type-1 NRG1 and GAPDH mRNAs were amplified in the presence of SYBR Green I. PCR amplification curves and difference in Ct were analyzed by a real-time temperature cycler (LightCycler, Roche Molecular Biochemicals). For figure display, RT-PCR products were also separated by agarose-electrophoresis and visualized with ethidium bromide staining.
doi:10.1371/journal.pone.0014185.g001

the transgene product than the Tg7 line. To confirm the overexpression of type-1 NRG1 mRNA in the transgenic mice, we carried out real-time quantitative reverse transcription (RT)-PCR for type-1 NRG1 mRNA in the presence of SYBR green I. Calculation of PCR amplification curves and the threshold cycle (Ct) suggested that the transgenic mice expressed approximately 4.3-fold (Tg5) and 2.2-fold (Tg7) higher levels of type-1 NRG1 mRNA than wild type littermates. The mRNA increases were also apparent in agarose gel electrophoresis (**Fig. 1D**).

The expression pattern of the GFP-NRG1 protein within the Tg5 line was examined by GFP-fluorescence. Under the control of the EF1 α promoter, GFP signals were ubiquitously and homogeneously distributed throughout the brain including the cerebral cortex, striatum, and hippocampus (**Fig. 2A-F**). There was a similar distribution pattern of GFP signals in the Tg7 line (data not shown).

Gross physical conditions of NRG1-Tg mice

The physical abilities of mice, such as sensory ability, motor reflex and coordination, directly and indirectly influence performance scores in behavioral tests. To estimate health and physical conditions of NRG1-Tg mice, we investigated various physical and behavioral parameters and compared between genotypes (transgenic vs wild), between lines (Tg5 vs Tg7) and between genders. MANOVA revealed that there was no significant main effect of genotype [$F(16, 30) = 1.249, P = 0.290$] or any significant interactions of genotype with line [$F(16, 39) = 0.974, P = 0.506$] or gender [$F(16, 39) = 118.50, P = 0.226$]. This suggests that the NRG1 transgene did not significantly influence gross health and physical conditions in NRG1-Tg mice. As MANOVA also detected significant main effects and/or interactions of gender and Tg line (see details in **Table S1** and **Table S2**), we analyzed two Tg lines independently and tested a gender x genotype interaction in the following individual behavioral tests.

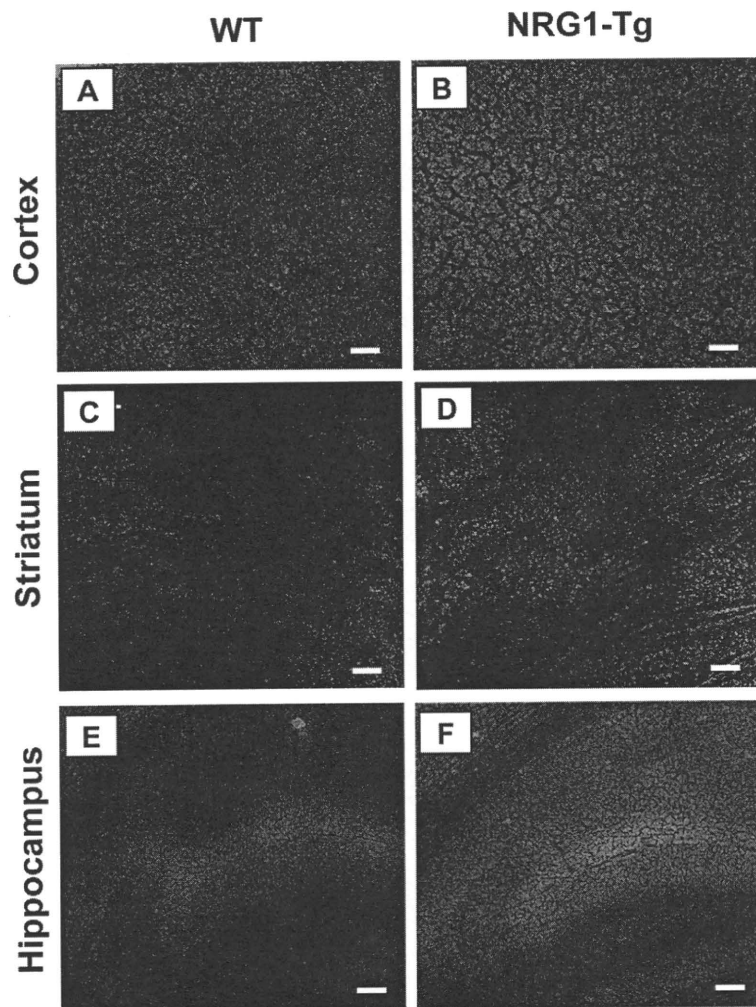


Figure 2. Detection of the transgene expression by GFP fluorescence in the brain. The transgenic line (NRG1-Tg5) was fixed and slices were prepared from their brain. The green fluorescence by GFP protein was examined in the cortex (**A, B**), striatum (**C, D**), and hippocampus (**E, F**), and compared between male NRG1-Tg and WT mice. Scale bars = 50 μ m in **A, B**, and 100 μ m in **C-F**. Note: Fixed brain of WT mice also exhibits autofluorescence but its intensity is lower than that of NRG1-Tg mice. doi:10.1371/journal.pone.0014185.g002

Hyperlocomotor activity of NRG1-Tg mice in a novel environment.

We assessed behavioral pathology of adult NRG1-Tg mice by measuring locomotor activity, prepulse inhibition (PPI), fear learning, and social interaction, which are often implicated in schizophrenia animal models. First, we used an open field task to examine the locomotor behavior of the NRG1 Tg lines, Tg5 and Tg7. A two-way repeated ANOVA using a between-subjects factor of genotype and a within-subjects factor of time revealed a significant main effect of genotype in both lines [Tg5: $F(1, 40) = 10.79, P < 0.05$; Tg7: $F(1, 27) = 5.19, P < 0.05$]. These results indicated that increases in NRG1 expression led to hyperactivity in a novel environment (**Fig. 3A, B**). The significant effect of time [Tg5: $F(11, 440) = 118.50, P < 0.001$; Tg7: $F(11, 297) = 25.03, P < 0.001$] and the lack of interaction between genotype and time [Tg5: $F(11, 440) = 0.60, P = 0.83$; Tg7: $F(11, 297) = 0.72, P = 0.72$] suggested that mice exhibited a decrease in locomotor activity over time. Furthermore, the rate of habituation was not significantly different between NRG1-Tg and WT mice. The novelty-induced rearing behavior of NRG1-Tg mice was simultaneously scored and compared with that of wild littermates. There were no significant differences in rearing behavior [genotype, Tg5: $F(1, 40) = 3.47, P = 0.07$; Tg7: $F(1, 27) = 2.17, P = 0.15$] (**Fig. 3C, D**).

NRG1-Tg mice exhibit normal prepulse inhibition and startle responses

Using different prepulse intensities, we examined and compared PPI levels of adult NRG1-Tg mice and WT littermates from the two Tg lines. Both NRG1-Tg mice revealed a non-significant trend toward decreasing PPI levels compared to WT mice [genotype, Tg5: $F(1, 39) = 3.39, P = 0.073$; Tg7: $F(1, 21) = 3.36, P = 0.081$]. PPI levels were dependent on prepulse intensity [Tg5: $F(3, 117) = 64.54, P < 0.001$; Tg7: $F(3, 63) = 76.9, P < 0.001$]. There was no significant interaction between genotype and prepulse intensity [Tg5: $F(3, 117) = 0.02, P = 0.99$; Tg7: $F(3, 63) = 0.05, P = 0.99$] (**Fig. 3E, F**). In pulse-alone startle responses, the amplitude of startle responses was dependent on pulse intensity [Tg5: $F(7, 140) = 90.14, P < 0.001$; Tg7: $F(7, 119) = 73.61, P < 0.001$]. There was no difference between the genotypes in both lines [genotype, Tg5: $F(1, 20) = 0.21, P = 0.65$; Tg7: $F(1, 17) = 0.06, P = 0.82$] and no significant interaction between genotype and tone intensity [Tg5: $F(7, 140) = 0.76, P = 0.62$; Tg7: $F(7, 119) = 1.15, P = 0.19$] (**Fig. 3G, H**).

Impaired context-dependent fear learning in NRG1-Tg mice

The effect of NRG1 overexpression on learning performance was examined in adulthood by measuring freezing behavior following fear conditioning. In this task, electric shock was coupled with a context plus a tone. In both mouse Tg lines, there was no significant difference in freezing rates during conditioning between NRG1-Tg mice and their WT littermates [genotype, Tg5: $F(1, 37) = 0.68, P = 0.42$; Tg7: $F(1, 21) = 0.05, P = 0.83$] (**Fig. 4A, B**). This finding suggests that there was no significant influence of the NRG1 transgene on shock sensitivities. A two-way repeated ANOVA using a between subjects factor of genotype and a within-subjects factor of time detected a significant effect of genotype on freezing rates when the test was coupled with the context [Tg5: $F(1, 37) = 8.45, P < 0.01$; Tg7: $F(1, 21) = 15.86, P < 0.01$]. However, there was no interaction between genotype and time [Tg5: $F(5, 185) = 0.66, P = 0.65$; Tg7: $F(5, 105) = 0.66, P = 0.65$] (**Fig. 4C, D**). In contrast, there was no significant difference in

tone-dependent learning between NRG1-Tg mice and their WT littermates [genotype, Tg5: $F(1, 37) = 1.84, P = 0.18$; Tg7: $F(1, 21) = 0.70, P = 0.41$] (**Fig. 4E, F**). These results indicate that the overexpression of NRG1 in the Tg mice specifically impairs context-dependent learning ability.

Social behavior of NRG1-Tg mice in an isolation-induced resident-intruder test

The effect of the NRG1 transgene on social behavior was examined using an isolation-induced resident-intruder test. In this assay, a resident male, who was previously housed alone, was exposed to an unfamiliar intruder male. The social (**Fig. 5A–D**) and aggressive behaviors (**Fig. 5E, F**) of the resident male in response to the intruder were monitored and scored. The NRG1-Tg residents displayed a significant decrease in the duration of social behaviors compared to those of WT male residents (anogenital sniffing, Tg5: $P < 0.05$; Tg7: $P < 0.05$; non-anogenital sniffing, Tg7: $P < 0.05$, non-agonistic social behavior, Tg5: $P < 0.01$; Tg7: $P < 0.01$, unpaired two tailed t-test) (**Fig. 5A, B**). There was no significant difference in non-anogenital sniffing between Tg5 and wild mice, however (non-anogenital sniffing, Tg5: $P = 0.13$, unpaired two tailed t-test). This trend was also supported by a decrease in the frequency of these behaviors (anogenital sniffing, Tg5: $P < 0.001$; Tg7: $P < 0.001$; non-anogenital sniffing, Tg5: $P = 0.42$; Tg7: $P < 0.05$; non-agonistic social behavior, Tg5: $P < 0.01$; Tg7: $P < 0.01$, unpaired two tailed t-test) (**Fig. 5C, D**). In aggressive behaviors, Tg5 male residents displayed an increase in frequency of aggressive following behavior ($P < 0.05$), but the frequency of attack and threat behaviors of Tg5 residents was indistinguishable from that of WT resident males (attack: $P = 0.39$; threat: $P = 0.90$) (**Fig. 5E**). In contrast, Tg7 resident males showed an increase in all indices of aggressive behaviors (aggressive following: $P < 0.05$ attack: $P < 0.01$; threat: $P < 0.05$) (**Fig. 5F**). Although the Tg line-specific behavioral changes require further investigation, our results from the resident-intruder test indicate that NRG1 overexpression has significant influences on social behavior.

Analysis of neurochemical markers for excitatory and inhibitory neurons and glial cells

NRG1 is involved in the regulation of GABAergic development, myelin formation, and NMDA receptor expression and function [23–26]. To explore whether the NRG1 transgene influenced these processes, we determined protein levels of molecular markers for GABAergic neurons, oligodendrocytes, and excitatory synapses and compared those between Tg5 mice and their WT littermates. Immunoblotting revealed that the immunoreactivity for parvalbumin, one of the phenotypic markers for cortical GABAergic neurons, was elevated in the frontal cortex of Tg5 mice ($P < 0.05$) (**Fig. 6A**). Furthermore, we also found significant increases in myelin-basic protein (MBP, $P < 0.01$) and 2',3'-cyclic nucleotide 3'-phosphodiesterase (CNPase, $P < 0.05$) in the same region (**Fig. 6A**). This result at least verified the hyper-signaling of NRG1 expressed from the transgene. There were no significant alterations in protein levels of glutamate decarboxylase (GAD) 65/67, NMDA receptor1 (NR1), and NMDA receptor 2A/2B (NR2A/2B) in the frontal cortex (**Fig. 6A**) as well as in all markers examined in other brain regions (**Fig. 6B, C**).

Analysis of dopaminergic markers, tissue contents of dopamine and its metabolites in NRG1-Tg mice

Recently we found that transient exposure of type-1 NRG1 protein to mouse pups produces persistent hyperdopaminergic

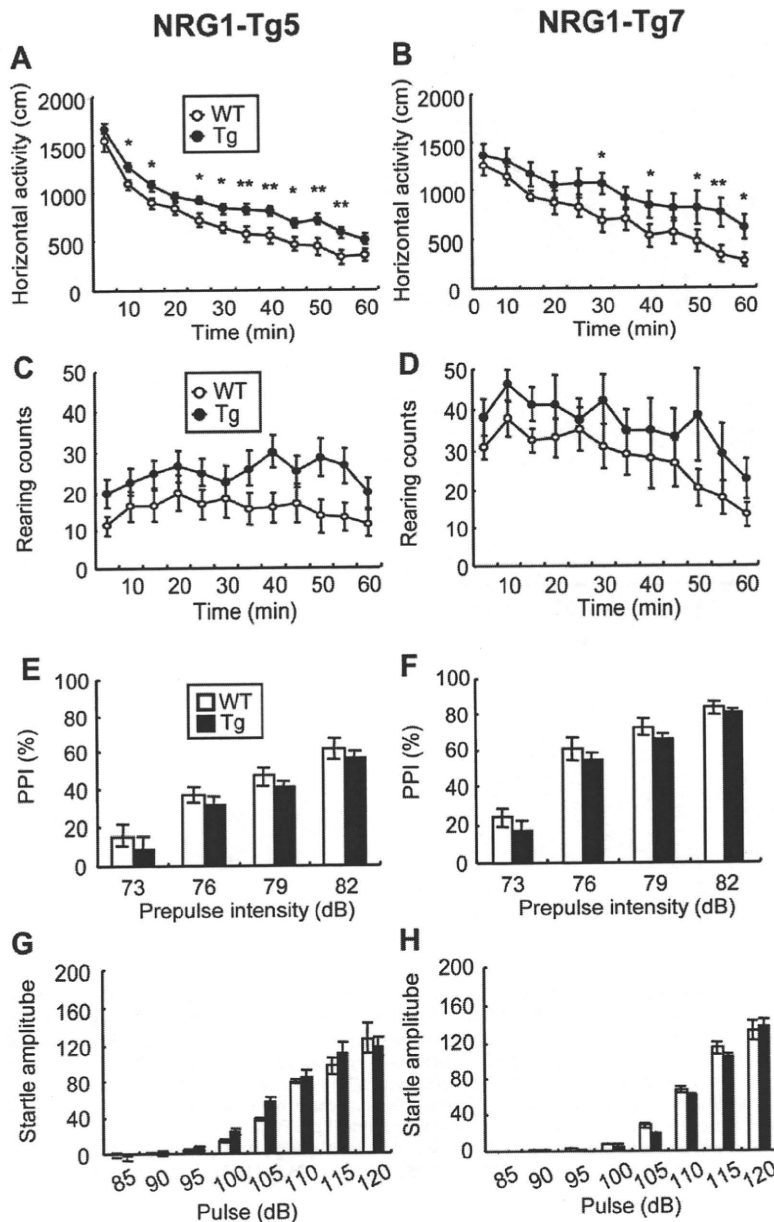


Figure 3. Locomotor activity and sensorimotor gating of NRG1-Tg mice. Behavioral traits were compared between NRG1-Tg5 mice and WT littermates (A, C, E, G) and between NRG1-Tg7 mice and WT littermates (B, D, F, H) at the adult stage (postnatal day PND 56–84). (A, B) Horizontal locomotor activity was scored every 5 min in a novel environment. (C, D) Rearing behavior was counted similarly [N=23 (male: N=9, female: N=14) for Tg5, N=18 (male: N=7, female: N=11) for WT; and N=15 (male: N=8, female: N=7) for Tg7, N=14 (male: N=6, female: N=8) for WT]. There was neither significant or marginal trend in a gender x genotype interaction; Tg5: $F(1, 37) = 1.06$ (locomotor activity) and 0.70 (rearing behavior), $P = 0.31$ (locomotor activity) and 0.79 (rearing behavior); Tg7: $F(1, 25) = 0.01$ (locomotor activity) and 0.11 (rearing behavior), $P = 0.94$ (locomotor activity) and 0.69 (rearing behavior). (E, F) Prepulse inhibition (PPI) percentages are shown with prepulses of 73, 76, 79 and 82 dB [N=23 (male: N=9, female: N=14) for Tg5, N=18 (male: N=7, female: N=11) for WT; and N=15 (male: N=8, female: N=7) for Tg7, N=14 (male: N=6, female: N=8) for WT]. There was neither significant or marginal trend in a gender x genotype interaction; Tg5: $F(1, 37) = 1.90$, $P = 0.18$; Tg7: $F(1, 19) = 0.11$, $P = 0.74$. (G, H) Relative amplitudes of startle responses to white noise at 75, 80, 85, 90, 95, 100, 105, 110, 115 and 120 dB tones are shown [N=12 (male: N=6, female: N=6) for Tg 5, N=10 (male: N=5, female: N=5) for WT; and N=10 (male: N=5, female: N=5) for Tg7, N=10 (male: N=5, female: N=5) for WT]. There was neither significant or marginal trend in a gender x genotype interaction; Tg5: $F(1, 18) = 0.64$, $P = 0.43$; Tg7: $F(1, 15) = 1.59$, $P = 0.23$. Data are expressed as mean \pm S.E.M. * $P < 0.05$, ** $P < 0.01$ compared to WT mice by Fisher's LSD. doi:10.1371/journal.pone.0014185.g003

states in the frontal cortex [27]. To assess the effects of NRG1 transgene on the dopamine system, we measured the levels of dopamine and its metabolites [dihydroxyphenylacetic acid (DO-

PAC) and homovanillic acid (HVA)] in various brain regions of adult mice. There were significant decreases in dopamine and DOPAC levels in the hippocampus of NRG1-Tg compared to

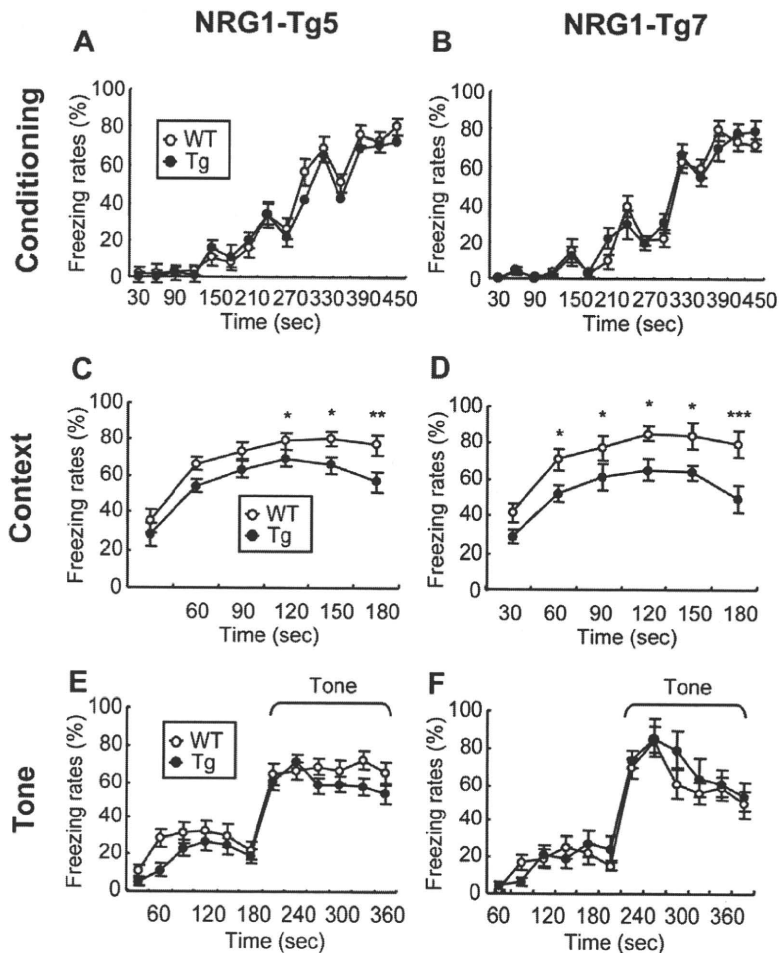


Figure 4. Context-dependent and tone-dependent fear learning in NRG1-Tg mice. Learning ability was compared between NRG1-Tg5 mice and WT littermates (**A, C, E**) and between NRG1-Tg7 mice and WT littermates (**B, D, F**). NRG1-Tg mice and WT littermates were subjected to shock-paired contextual conditioning with a tone cue. One day after conditioning, their learning performance was measured in the presence of a contextual or tone cue. (**A, B**) Freezing rates (time %) were compared between NRG1-Tg mice and WT littermates during conditioning. (**C, D**) Freezing rates during context exposure are shown. (**E, F**) Freezing rates were compared between NRG1-Tg mice and WT littermates during tone exposure [N=21 (male: N=11, female: N=10) for Tg5, N=18 (male: N=10, female: N=8) for WT; and N=12 (male: N=6, female: N=6) for Tg7, N=11 (male: N=6, female: N=5) for WT]. There was neither significant or marginal trend in a gender \times genotype interaction; Tg5: $F(1, 35) = 0.06$ (conditioning), 0.01 (context) and 0.19 (tone), $P=0.81$ (conditioning), 0.99 (context) and 0.66 (tone); Tg7: $F(1, 19) = 0.01$ (conditioning), 0.10 (context) and 0.91 (tone), $P=0.94$ (conditioning), 0.76 (context) and 0.35 (tone). Data are expressed as mean \pm S.E.M. * $P<0.05$, ** $P<0.01$, *** $P<0.001$ compared to WT mice by Fisher's LSD.

doi:10.1371/journal.pone.0014185.g004

WT mice (dopamine: $P<0.01$; DOPAC: $P<0.001$) although there were no differences in the HVA ($P=0.12$) (**Fig. 7C**). In the frontal cortex, there was a trend toward decreasing dopamine content of NRG1-Tg mice, but not statistically significant (dopamine: $P=0.065$; DOPAC: $P=0.19$; HVA: $P=0.41$) (**Fig. 7A**). In the striatum, there were no differences in the dopamine and its metabolites (dopamine: $P=0.20$; DOPAC: $P=0.54$; HVA: $P=0.88$) (**Fig. 7B**).

To explore the molecular mechanism underlying the changes in dopaminergic metabolism, we examined the protein markers related to dopamine synthesis and transmission [tyrosine hydroxylase (TH), dopamine beta hydroxylase (DBH), dopamine transporter (DAT), D1 dopamine receptor (D1DR), D2 dopamine receptor (D2DR), and vesicular monoamine transporter (vMAT2)] in the frontal cortex, hippocampus and striatum. In agreement with the above change in dopamine metabolism, we found a significant

protein decrease in TH, a rate-limiting enzyme of dopamine and noradrenaline synthesis, in the hippocampus ($P<0.05$) (**Fig. 7E**). The decrease in TH levels was manifested in the frontal cortex as well. In addition, we found significant increase in D2DR protein levels in the frontal cortex (**Fig. 7D**). To assess the influence on noradrenergic terminals, we also determined protein levels of dopamine- β -hydroxylase (DBH), the enzyme that converts dopamine to noradrenaline. There was no significant change in DBH levels in the frontal cortex and hippocampus (**Fig. 7D, F**). We also failed to detect significant alteration in DAT, D1DR, vMAT2 in all the regions examined (**Fig. 7D-F**). These results suggest that the life-long increase in NRG1-expression disrupts dopaminergic synthesis and transmission in the cortico-limbic system. The present phenomenon contrasts our recent finding that neonatal treatment with NRG1 protein enhances dopamine synthesis and release in adulthood [27].

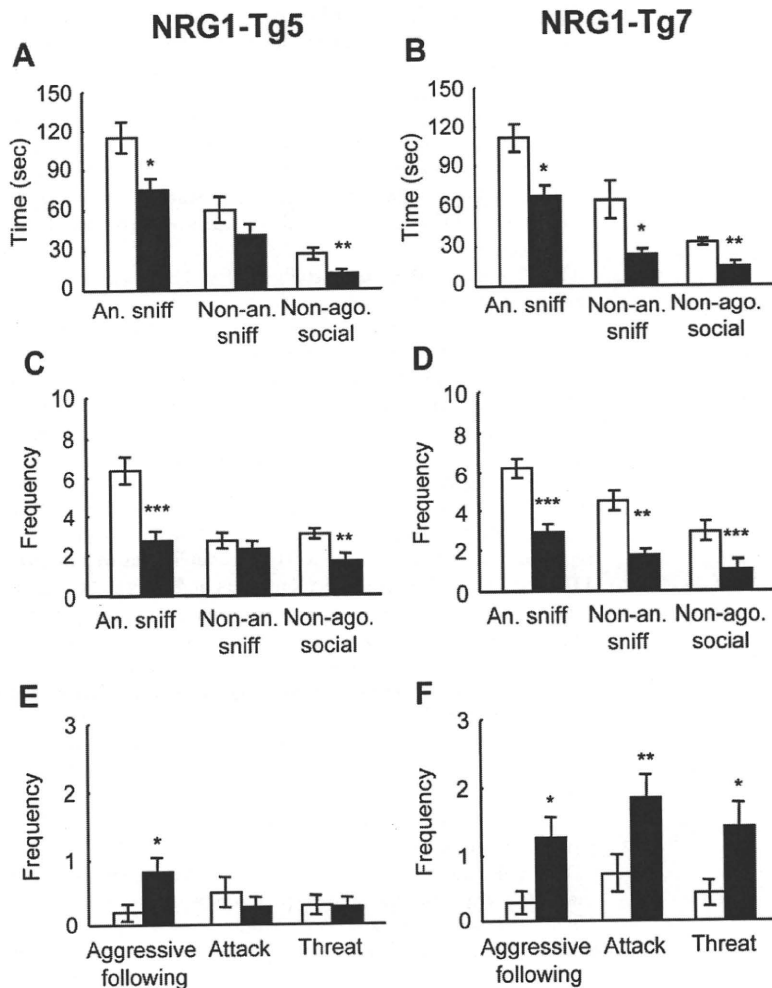


Figure 5. Isolation-induced resident-intruder test. NRG1-Tg5 mice (A, C, E) and Tg7 mice (B, D, F) and their WT littermates were subjected to a isolation-induced resident-intruder test. (A–D) Social scores of anogenital sniffing (An. sniff), non-anogenital sniffing (Non-an. sniff) and non-agonistic social behaviors (Non-ago. social) were measured over a 10-min period. The non-agonistic behaviors represent grooming and lying down next to each other of resident mice. (E, F) Aggressive behaviors, which represent aggressive following, attacks and threats, were counted in parallel. (A, B) Time spent by the resident males actively pursuing social behaviors. (C, D) The frequency of social behaviors in the resident males is shown. (E, F) The frequency of aggressive behaviors of the resident males was compared between the NRG1-Tg mice and their WT littermates (N=11 for Tg5, N=10 for WT; and N=7 for Tg7, N=7 for WT, all males). Data are expressed as mean±S.E.M. * $P<0.05$, ** $P<0.01$, *** $P<0.001$ compared to WT littermates by unpaired two-tailed t-test. doi:10.1371/journal.pone.0014185.g005

Discussion

To investigate the neurobehavioral consequences of life-long NRG1 hyper-signaling, we established Tg mouse lines carrying the GFP-tagged-NRG1 (type-1) cDNA driven by the ubiquitous transcription promoter. We selected two Tg lines and backcrossed those lines with C57BL/6N mice (more than seven times) to stabilize the transgene in a single genomic integration site. One of the lines carried more copies of the NRG1 transgene than the other. In agreement, the expression of the transgene was higher in the Tg5 line compared to the Tg7 line as shown by immunoblotting as well as by real time RT-PCR. Our results indicated that the expression of the NRG1 transgene was widespread throughout the brain. As indicated the neurotrophic actions of this neurotrophic factor, the Tg mice exhibited the increase in the phenotypic markers of GABAergic neurons and oligodendrocytes [14], [15], [23], [24], [28]. In spite of

the reported neurotrophic activity of NRG1 on midbrain dopaminergic neurons [29], [30], the hippocampal decrease in TH and dopamine was observed beyond our expectation.

These two independent Tg mouse lines displayed similar levels of neurobehavioral abnormalities; hyper-locomotor activity in a novel environment, learning deficits in context-fear conditioning, reduced social interactions, and a nonsignificant trend toward decreasing prepulse inhibition. Both lines also exhibited the normal behavioral phenotypes that were indistinguishable from WT littermates in acoustic startle amplitudes, vertical movement, shock sensitivity, and tone-dependent fear learning. These behavioral traits of the Tg mice appear to indicate their normal motor function or sensory abilities in a limited degree. We do not exclude the possibility that unexamined physical functions, such as olfaction, might be altered by NRG1 overexpression and influence social interaction scores of the Tg mice.

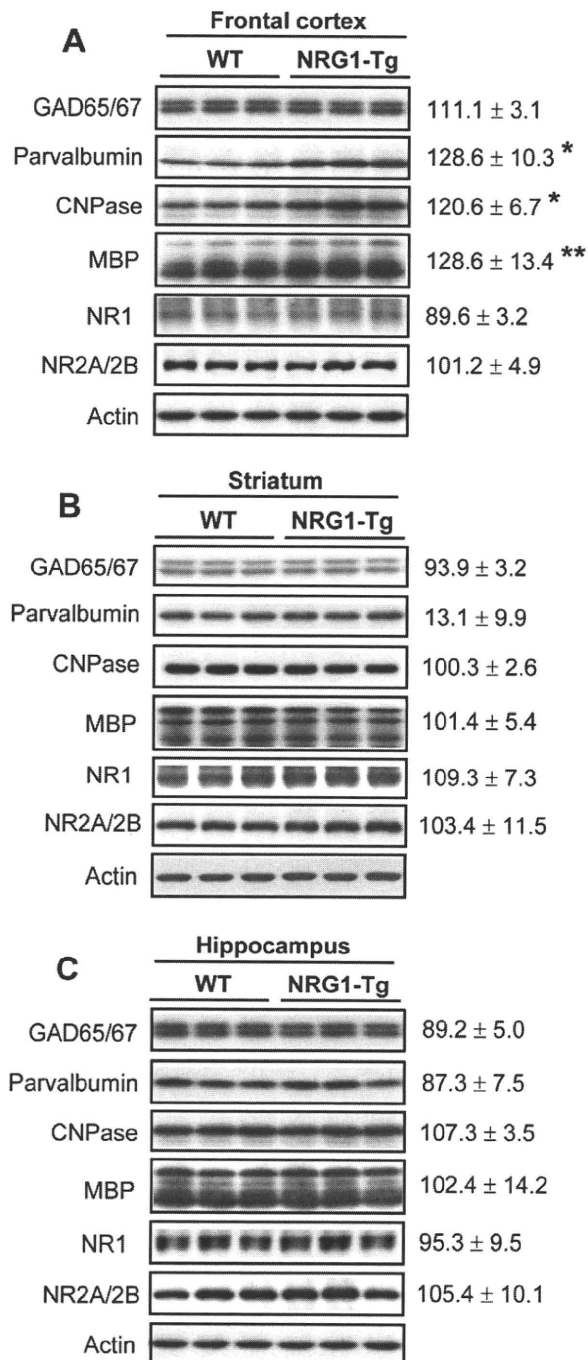


Figure 6. The expression of GABA-, myelin-, and excitatory synapse-associated molecular markers. Protein extract was prepared from (A) frontal cortex, (B) striatum, and (C) hippocampus and subjected to immunoblotting with antibodies directed against the GABAergic markers (GAD65/67 and parvalbumin), oligodendrocyte markers (CNPase and MBP), and excitatory synaptic markers (NR1 and NR2A/2B). Immunoreactivity on immunoblots was measured by densitometric analysis, and normalized to β -actin levels. Percentage ratio to that of WT littermates was calculated (mean \pm S.E.M, N = 5, all males) and analyzed by unpaired two-tailed t-test. doi:10.1371/journal.pone.0014185.g006

The behavioral homology between these two independent Tg lines presumably rules out the possibility that genomic disturbance of the transgene integration was involved in these behavioral deficits. In addition, it is also unlikely that the distinct genome background impurities of the two independent Tg lines resulted in the same behavioral traits. In this context, the discordant behavioral trait (social aggression) between the two Tg lines might be illustrated by the distinct genomic disturbance of the transgene integration or different background impurities of the original DBA mouse genome.

The Tg mice in the present study displayed both an increase in horizontal locomotor activity and a decrease in social behavior. Interestingly, hyperlocomotion is typically associated with positive symptoms in a mouse model of schizophrenia whereas reduced social activity is implicated as a negative symptom of this illness [31–33]. The hypo-dopaminergic state is often associated with impairments in social and learning behaviors, and might illustrate some of the behavioral traits of the present transgenic mice [34], [35]. In particular, their hypo-dopaminergic state in the limbic system might impair the hippocampal functions, leading to their context learning deficits [35]. The observed behavioral traits are reported in studies of various NRG1 knockout lines as well [5], [8–11]. Although we failed to detect significant and marginal gender \times genotype interactions in individual behavioral tests, the physical examination test detected a significant main effect of gender and an interaction between Tg line and gender, presumably suggesting the dose-dependent NRG1 effects on gender-specific behavioral trends. This agrees with the reports that the down-regulation of NRG1-ErbB signaling in mice exhibit sexually dimorphic changes in several behavioral paradigms such as exploratory and habituation profiles [8], [36], [37]. The biological mechanism underlying the interaction between sex hormone and NRG1 signaling remains to be studied.

Unexpectedly, the present study and previous reports indicate that both hypomorphic and hypermorphic expression of the NRG1 gene may produce several common behavioral phenotypes in mice. This finding is quite surprising but raises a challenging question about the molecular and cellular mechanisms underlying the behavioral deficits common to both the hypermorphic and hypomorphic expression of NRG1.

PPI is also implicated in the neuropathology of schizophrenia and its animal models. In contrast to the abnormality in social behavior or locomotor activity, the PPI deficits of these Tg mice appear to be moderate. The NRG1 knockout line (transmembrane-domain of NRG1^{+/−}) similarly displayed moderate or non-significant abnormality in PPI levels [2], [13]. Since there are variations in the magnitude of PPI deficits depending upon the targeted exon of NRG1 gene [4], the behavioral phenotype of the present NRG1-Tg mice is not discordant with that of NRG1 knockout mice in this context. The recent report is noteworthy that the specific overexpression of type-1 NRG1 driven by a Thy-1 promoter in brain projection neurons markedly impairs PPI [38]. The use of distinct gene promoters of EF1 α and Thy-1 genes differentially regulates timing and cell types of the transgene expression and presumably results in the difference in mouse behavior. Controversy of the behavioral difference between these NRG1 Tg lines awaits further investigations, however.

NRG1 is one of the neurotrophic factors that positively regulate neuronal migration, synaptogenesis, GABAergic and dopaminergic neuronal development, and myelination [14], [15], [27–30], [39–41]. In agreement with the given biological activities of NRG1, we found the increases in parvalbumin, MBP and CNPase. These molecular phenotypes of the NRG1-Tg mice well contrast those of NRG1 knockout mouse lines. ErbB4, the

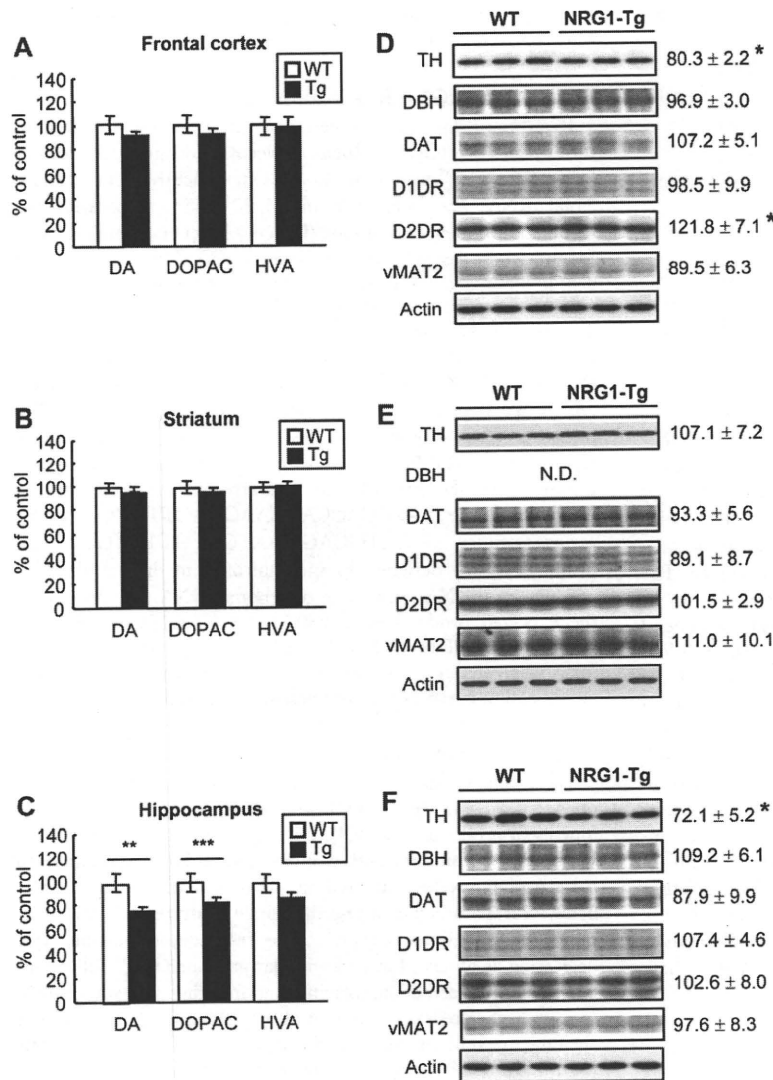


Figure 7. Analysis of dopamine metabolism and neurochemical markers for dopaminergic neurons of NRG1 transgenic mice. Levels of dopamine and its metabolites (DOPAC and HVA) (A, B, C) as well as those of dopamine-related molecular markers (D, E, F) were measured in (A, D) frontal cortex, (B, E) striatum and (C, F) hippocampus of NRG1-Tg5 and WT mice at the adult stage. Typical immunoblots for TH, DBH, DAT, D1DR, D2DR, and vMAT2 were displayed. Each immunoreactivity was measured by densitometric analysis, normalized to β -actin levels and its ratio to that of WT littermates was displayed (N=4–5 each, all males). Data are expressed as mean \pm S.E.M. (% of WT). * P <0.05, ** P <0.01, *** P <0.001, compared to WT littermates by unpaired two-tailed t-test. doi:10.1371/journal.pone.0014185.g007

receptor for NRG1 knockout-mutants exhibit reduced parvalbumin positive cells in the hippocampus [28] and loss of ErbB4 signaling by its dominant-negative form reduced oligodendrocyte number and myelination [41]. These phenotypic abnormalities of NRG1 knockout mice are in agreement with the neuropathological findings on postmortem brains of schizophrenia patients [42–44]. Conversely, the present NRG1-Tg mice, which display the increases in these pathological markers, may be irrelevant to an animal model for schizophrenia in spite of their schizophrenia-like behavioral deficits. In this context, it is a challenging question how the hyper-NRG1 signals reported in patients' postmortem brains is associated with the above neuropathologic deficits.

NRG1 is reported to promote cell survival of midbrain dopaminergic neurons and trigger dopamine release [29], [30],

[45–47]. Accordingly, we had expected positive influences of the NRG1 transgene expression on the dopaminergic system in the present experiment. However, the direction of the dopaminergic changes in NRG1-Tg mice was opposite to our expectation. NRG1-Tg mice rather displayed reduction in TH protein levels and dopamine content in the hippocampus and/or frontal cortex. It is a challenging question how the hyper-signaling of NRG1 produced the TH decrease. This discrepancy might be illustrated by the NRG1 action on dopaminergic neurons [46]. NRG1 evokes an almost immediate overflow of striatal dopamine when injected into a region just dorsal to the substantia nigra. Therefore, it is possible that the life-long hyper signals of NRG1 might result in constant dopamine over-flow and produce cytotoxic influences on dopaminergic terminals [48], [49]. As there are many alternative

explanations for this controversy, the exact mechanism underlying this phenomenon remains to be explored.

In summary, our behavioral results from NRG1-Tg mice and previous findings on NRG1 knockout mice highlight the complex dose dependency of NRG1 functioning in brain development or behavioral regulation.

Materials and Methods

Ethics statement

All of the animal experiments described were approved by the Animal Use and Care Committee guidelines of Niigata University and performed in accordance with the guidelines of NIH (USA).

Generation of NRG1-Tg mice

The GFP gene was inserted into the NspV-SacI site between the immunoglobulin (Ig)-like and epidermal growth factor (EGF)-like domains of NRG1 β 1 cDNA [50]. The 2.6 kb cDNA fragment encoding mouse NRG1 β 1 and GFP tag was then excised by EcoRI-XbaI digestion, subcloned into the EcoRI-XbaI site of a mammalian vector pT113 (gifted from Dr. Shigekazu Nagata, Osaka University) and ligated to an EF-1 α gene promoter. The DNA construct of the transgene was confirmed by DNA sequencing (data not shown). Transgenic mice were generated by pronuclear injection of the fragment (shown in **Fig. 1A**) into fertilized mouse eggs (DBA/2 \times C57BL/6 F1). The lines of the NRG1-Tg mice (Tg5 and Tg7, chosen for its low copy number of the transgene) were backcrossed with C57BL6Ncr mice (purchased from Nihon Charles River, Yokohama, Japan) for 7–9 generations, and their offspring of heterozygous mice was used in this study. Mice were genotyped by PCR using primers corresponding to the Ig-like domain of NRG1 (forward: 5'-TGCCTCCAGATTGAAAGAG) and the EGF domain of NRG1 (reverse: 5'-TTCTCCTTCTCCGCACACTT), giving a product with 1112 bp. All Tg mice were bred and housed under a 12 h light-dark cycle with free access to food and water. The mice were subjected to behavioral testing during the light phase between postnatal day (PND) 56–84.

Immunoblotting

Whole brain tissues were homogenized in lysis buffer (62.5 mM Tris-HCl pH 6.8, 2% SDS, 0.5% NP-40, 5 mM EDTA) with a protease inhibitor cocktail (Roche, Indianapolis, IN, USA). After centrifugation, the supernatant was collected and protein concentrations were determined. Equal amounts of protein (30 μ g/lane) were subjected to sodium dodecyl sulfate–polyacrylamide gel electrophoresis and transferred to nitrocellulose membranes. The membranes were incubated with anti-extracellular-NRG1 (7D5, 1:1000, NeoMarkers, Fremont, CA, USA) or anti-GFP (1:2000, Clontech, Palo Alto, CA, USA) monoclonal antibodies. Alternatively, immunoblots were probed with anti-GAD 65/67 (1:5000, Sigma-Aldrich, St Louis, MO, USA), anti-parvalbumin (1:10000, Abcam, Cambridge, UK), anti-MBP (1:1000, Millipore, Bedford, MA, USA), anti-CNPase (1:1000, Millipore), anti-NR1 (1:250, Millipore), anti-NR2A/B (1:150, Millipore), and anti- β -actin (1:4000, Millipore) antibodies. Immunoblots were alternatively probed with antibodies directed against the following dopamine-related molecules; TH (1:1000, Millipore), DBH (1:1000, Millipore), DAT (1:1000, Millipore), D1DR (1:500, Santa Cruz Biotechnology, Santa Cruz, CA, USA), D2DR (1:250, Millipore), and vMAT2 (1:1000, Millipore). Immunoreactivity was detected by peroxidase-conjugated anti-rabbit or peroxidase-conjugated anti-mouse Ig antibody followed by a chemiluminescence reaction

combined with X-ray film exposure (ECL kit; GE Healthcare, Little Chalfont, UK).

Analysis of NRG1 mRNA expression

Real-time RT-PCR was performed in a fluorescent temperature cycler (LightCycler, Roche Molecular Biochemicals, Mannheim, Germany) according to the manufacturer's instruction. Total RNA was isolated from whole brain tissue with the guanidinium-phenol solution (Isogen, Nippon Gene, Osaka, Japan) and treated with DNase I (20 U/ml) to remove contaminating genomic DNA. NRG1 mRNA was detected by recombinant *Thermus thermophilus* DNA polymerase (High-Plus, Toyobo, Osaka, Japan) using the forward primer (5'-GCAAGGAGGAGGCAAG) and the reverse primer (5'-GCTACGGTTCAGCTCATTCC), which correspond to exon 2 and exon 3 sequences of mouse NRG1 genome, respectively. The primer set was designed to amplify mRNA transcripts specific for type-1 NRG1. RT-PCR of glyceraldehyde-3-phosphate dehydrogenase (GAPDH) mRNA was similarly carried out with the forward primer (5'-TGCACCACCAACTGCTTAGC) and the reverse primer (5'-GATGCAGGGATGATGTTCTG). These primer sets were designed to span intron(s) to distinguish PCR products of mRNA from those of genomic DNA. The lengths of the expected products were 230 bp for NRG1 β 1 mRNA and 239 bp for GAPDH mRNA. The genome copy number of the Tg mice was estimated by the comparative Ct method using the amplification curve of the wild genome as a standard [51].

Physical examinations

We employed the primary behavioral screen SHIRPA developed by Rogers et al. [52] and estimate a behavioral and functional profile of NRG1 Tg mice by observational assessment. Parameters of undisturbed animals and animals submitted to battery of reflex tests are scored for quantitative analysis. The behavioral parameters assessed include posture, activity, gait, motor coordination, tremor, startle response, excitability and defecation as observed in a viewing jar and open field. Salivation, lacrimation, piloerection, placing and righting reflexes, muscle tone and other reflexes were scored by picking the animal up and eliciting the reflexes with specific equipment and manipulations [53], [54]. Naïve mice (i.e., mice not exposed to any other behavioral test) were used for these physical examinations.

Analysis of Locomotor Activity

Exploratory motor activity was measured in a novel environment under dim light. Mice were placed in an automated activity apparatus (27 cm L \times 27 cm W \times 20 cm H, MED Associates, St. Albans, VT, USA) equipped with infrared photosensors at 1.62 cm intervals, and we measured horizontal activity every 5 min for the first hour [27]. Horizontal activity was assessed via beam crossings, which were counted by a fully automated tracking system (Activity Monitor, Med Associates).

Measurement of acoustic startle response and prepulse inhibition

Mice were placed in a plastic cylinder and fixed in an automated startle chamber (SR-Lab Systems, San Diego, CA, USA) [27]. After a 5-min acclimation period with 70-dB background noise (white noise), an 75-, 80-, 85-, 90-, 100-, 110-, or 120-dB white noise stimulus (40 msec duration) was given 8 times to each mouse in the same pseudo-random order at 15 sec intervals. Analysis for startle amplitudes was based on the mean of the seven trials (ignoring the first trial) for each trial type. PPI

responses were measured with 120 dB acoustic stimuli combined with four different prepulse intensities. Each mouse was placed in the startle chamber (SR-Lab) and initially acclimatized for 5 min with background noise alone (70 dB white noise). The mouse was then subjected to 48 startle trials, each trial consisting of one of six conditions: (i) a 40 msec 120 dB noise burst presented alone, (ii–v) a 40 msec 120 dB noise burst following prepulses by 100 msec (20 msec noise burst) that were 3-, 6-, 9-, or 12-dB above background noise (i.e., 73-, 76-, 79-, or 82-prepulse, respectively), or (vi) no stimulus (background noise alone), which was used to measure baseline movement in the chamber. These six trial types (i–vi) were each repeated 8 times in a pseudorandom order to give 48 trials. The inter-trial interval was 15 sec. Each trial type was presented once within a block of six trials and the order of 48 trial presentations was fixed for all mice. Analysis was based on the mean of the seven trials for each trial type. The percentage PPI of a startle response was calculated as: $100 - [(startle\ response\ on\ prepulse-pulse\ stimulus\ trials - no\ stimulus\ trials) / (pulse-alone\ trials - no\ stimulus\ trials)] \times 100$.

Context- and tone-dependent fear learning

The test paradigm for contextual fear conditioning was modified from procedures published in Frankland et al, 2004 [55]. Mice were placed in a shock chamber with a grid floor (10 cm L×10 cm W×10 cm H; Obaraika Ltd. Tokyo, Japan), and their baseline movement/freezing behavior was monitored for 2 min. The mice were then exposed to three rounds of 0.8 mA electric shocks (2 sec duration) with 180 sec tone cues (60 dB, 10 kHz). One day after conditioning, mice were returned to the chamber. The time spent freezing (i.e., no movement other than respiration) was recorded and scored at 30 sec intervals for 3 min. After 3 h, the mice were moved to a different chamber with a flat floor (10 cm L×10 cm W×10 cm H). In this chamber, the time spent freezing was recorded and scored for 3 min before and after the tone cue. Freezing behavior was monitored by a video camera during all sessions and analyzed by imaging software (Obaraika Ltd.).

Isolation-induced resident-intruder test

The isolation-induced resident-intruder test to estimate social behaviors was modeled after the procedure described by Mohn et al, 1999 [56]. For one week before testing, male wild-type (WT) and NRG1-Tg mice were housed individually (resident) or in groups (intruder) of three or four mice. We note that the bedding was changed in all cages one day prior to testing. On the test day, an intruder was placed in the home cage of resident mice, and their behavior was video-recorded for 10 min. The duration and frequency of 1) anogenital sniffing, 2) sniffing of any part of resident mice excluding anogenital area (non-anogenital sniffing) and 3) non-agonistic social behaviors (grooming and lying down next to each other of resident mice) were scored by observers blind to the experimental conditions. In addition, aggressive behaviors; 1) aggressive following (resident mice rapidly follow intruder mice from behind and force it to retreat, fiercely tugging hair or tail), and 2) attacks (biting and pinning), and 3) threats (upright posture and tail rattling) were scored. Scores for each behavior were then averaged for each genotype. The experimental groups included 10 WT residents and 11 NRG1-Tg residents in the Tg5 line experiment, and 7 WT and 7 NRG1-Tg residents in the Tg7 line experiment. We purchased and used novel adult male C57BL/6 NCr mice (same age) as unfamiliar intruders.

Quantification of dopamine and its metabolites

We measured the tissue contents of dopamine, DOPAC and HVA as described previously [57]. The prefrontal cortex, hippocampus, and striatum were dissected and frozen on dry ice. The tissue was homogenized in monoamine extraction buffer [0.1 M perchloric acid, 0.1 mM EDTA, 50 nM isoproterenol (internal standard)], incubated on ice for 30 min, and then centrifuged at 10,000×g for 10 min. Precipitates were homogenized in 0.5 N NaOH for protein determination.

The high performance liquid chromatography (HPLC) system consisted of a pump (model LC-10ADVP; Shimadzu, Kyoto, Japan), an automatic sample injector (model SIL-10ADVP; Shimadzu), and an electrochemical detector (ECD) with a glassy carbon-working electrode (model ECD-300; Eicom, Kyoto, Japan). Tissue contents of dopamine, DOPAC and HVA were measured using a C18 column (model CA-5ODS, 4.6×150 mm; Eicom). The mobile phase consisted of 50 mM trisodium citrate, 25 mM NaH₂PO₄, 0.03 mM EDTA, 10 mM diethylamine, 3 mM octanesulfonic acid sodium salt, 6% methanol, and 1% dimethylacetamide, pH 3.2.

Statistical analysis

Health and physical conditions (39 parameters) were analyzed using a multiple analysis of variance (MANOVA) with genotype (two levels), line (two levels) and gender (two levels). Behavioral scores were initially analyzed using a three-way analysis of variance (ANOVA) with genotype (two levels) and gender (two levels) as the between-subjects factors and time or prepulse (four levels) as the within-subjects factors. Because the initial ANOVAs did not yield any significant results with gender, the variable was collapsed and the analysis rerun. Univariate data for the social behavioral scores, protein expression levels and monoamine contents were analyzed using an unpaired two-tailed *t* test. For post hoc testing, Fisher's LSD was used to detect differences in the absolute behavioral values. A *P*-value of less than 0.05 was regarded as statistically significant, and "N" values represent the number of animal used in the analysis. These statistical analyses were performed using SPSS 11.0 for Windows.

Supporting Information

Table S1. Statistical values and results of MANOVA in SHIRPA test. N, animal number; AVE, average; SD, standard deviation.

Found at: doi:10.1371/journal.pone.0014185.s001 (0.03 MB DOC)

Table S2. Physical and health conditions of NRG1-Tg mice in SHIRPA test. N, animal number; AVE, average; SD, standard deviation.

Found at: doi:10.1371/journal.pone.0014185.s002 (0.05 MB DOC)

Acknowledgements

The authors are grateful to Minoru Tanaka and Sachiko Hirokawa for mouse breeding.

Author Contributions

Conceived and designed the experiments: HN. Performed the experiments: TK AK MM LF MY. Analyzed the data: TK AK SM. Contributed reagents/materials/analysis tools: NS SM MY MO. Wrote the paper: TK HN.

References

- Stefansson H, Sarginson J, Kong A, Yates P, Steinthorsdottir V, et al. (2003) Association of neuregulin 1 with schizophrenia confirmed in a Scottish population. *Am J Hum Genet* 72: 83–87.
- Stefansson H, Sigurdsson E, Steinthorsdottir V, Bjornsdottir S, Sigmundsson T (2002) Neuregulin 1 and susceptibility to schizophrenia. *Am J Hum Genet* 71: 877–892.
- Li D, Collier DA, He L (2006) Meta-analysis shows strong positive association of the neuregulin 1 (NRG1) gene with schizophrenia. *Hum Mol Genet* 15: 1995–2002.
- Chen YJ, Johnson MA, Lieberman MD, Goodchild RE, Schobel S, et al. (2008) Type III neuregulin-1 is required for normal sensorimotor gating, memory-related behaviors, and corticostriatal circuit components. *J Neurosci* 28: 6872–6883.
- Ehrlichman RS, Luminais SN, White SL, Rudnick ND, Ma N, et al. (2009) Neuregulin 1 Transgenic Mice Display Reduced Mismatch Negativity, Contextual Fear Conditioning and Social Interactions. *Brain Res* 1294: 116–127.
- Gerlai R, Pisacane P, Erickson S (2000) Heregulin, but not ErbB2 or ErbB3, heterozygous mutant mice exhibit hyperactivity in multiple behavioral tasks. *Behav Brain Res* 109: 219–227.
- Karl T, Duffy L, Scimone A, Harvey RP, Schofield PR (2007) Altered motor activity, exploration and anxiety in heterozygous neuregulin 1 mutant mice: implications for understanding schizophrenia. *Genes Brain Behav* 6: 677–687.
- O'Tuathaigh CM, O'Sullivan GJ, Kinsella A, Harvey RP, Tighe O, et al. (2006) Sexually dimorphic changes in the exploratory and habituation profiles of heterozygous neuregulin-1 knockout mice. *Neuroreport* 17(1): 79–83.
- O'Tuathaigh CM, Babovic D, O'Meara G, Clifford JJ, Croke DT, et al. (2007a) Susceptibility genes for schizophrenia: characterisation of mutant mouse models at the level of phenotypic behaviour. *Neurosci Biobehav Rev* 31(1): 60–78.
- O'Tuathaigh CM, Babovic D, O'Sullivan GJ, Clifford JJ, Tighe O, et al. (2007b) Phenotypic characterization of spatial cognition and social behavior in mice with 'knockout' of the schizophrenia risk gene neuregulin 1. *Neuroscience* 147: 18–27.
- O'Tuathaigh CM, O'Connor AM, O'Sullivan GJ, Lai D, Harvey R, et al. (2008) Disruption to social dyadic interactions but not emotional/anxiety-related behaviour in mice with heterozygous 'knockout' of the schizophrenia risk gene neuregulin-1. *Prog Neuropsychopharmacol Biol Psychiatry* 32(2): 462–466.
- Rimer M, Barrett DW, Maldonado MA, Vock VM, Gonzalez-Lima F (2005) Neuregulin-1 immunoglobulin-like domain mutant mice: clozapine sensitivity and impaired latent inhibition. *Neuroreport* 16: 271–275.
- Van den Buuse M, Wischhof L, Xi Lec R, Martin S, Karl T (2009) Neuregulin 1 hypomorphic mutant mice: enhanced baseline locomotor activity but normal psychotropic drug-induced hyperlocomotion and prepulse inhibition regulation. *Int J Neuropsychopharmacol* 29: 1–11.
- Harrison PJ, Law AJ (2006) Neuregulin 1 and schizophrenia: genetics, gene expression, and neurobiology. *Biol Psychiatry* 60: 132–140.
- Mei L, Xiong WC (2008) Neuregulin 1 in neural development, synaptic plasticity and schizophrenia. *Nat Rev Neurosci* 9: 437–452.
- Hashimoto R, Straub RE, Weickert CS, Hyde TM, Kleinman JE, et al. (2004) Expression analysis of neuregulin-1 in the dorsolateral prefrontal cortex in schizophrenia. *Mol Psychiatry* 9: 299–307.
- Law AJ, Lipska BK, Weickert CS, Hyde TM, Straub RE, et al. (2006) Neuregulin 1 transcripts are differentially expressed in schizophrenia and regulated by 5' SNPs associated with the disease. *Proc Natl Acad Sci U S A* 103: 6747–6752.
- Petryshen TL, Middleton FA, Kirby A, Aldinger KA, Purcell S, et al. (2005) Support for involvement of neuregulin 1 in schizophrenia pathophysiology. *Mol Psychiatry* 328: 366–74.
- Lachman HM, Pedrosa E, Nolan KA, Glass M, Ye K, et al. (2006) Analysis of polymorphisms in AT-rich domains of neuregulin 1 gene in schizophrenia. *Am J Med Genet B Neuropsychiatr Genet* 141B(1): 102–9.
- Chong VZ, Thompson M, Beltaifa S, Webster MJ, Law AJ, et al. (2008) Elevated neuregulin-1 and ErbB4 protein in the prefrontal cortex of schizophrenic patients. *Schizophr Res* 100: 270–280.
- Hahn CG, Wang HY, Cho DS, Talbot K, Gur RE, et al. (2006) Altered neuregulin 1-erbB4 signaling contributes to NMDA receptor hypofunction in schizophrenia. *Nat Med* 12: 824–828.
- Ozaki M, Itoh K, Miyakawa Y, Kishida H, Hashikawa T (2004) Protein processing and releases of neuregulin-1 are regulated in an activity-dependent manner. *J Neurochem* 91: 176–88.
- Brinkmann BG, Agarwal A, Sereda MW, Garratt AN, Müller T, et al. (2008) Neuregulin-1/ErbB signaling serves distinct functions in myelination of the peripheral and central nervous system. *Neuron* 59: 581–595.
- Flames N, Long JE, Garratt AN, Fischer TM, Gassmann M, et al. (2004) Short- and long-range attraction of cortical GABAergic interneurons by neuregulin-1. *Neuron* 44: 251–261.
- Li B, Woo RS, Mei L, Malinow R (2007) The neuregulin-1 receptor erbB4 controls glutamatergic synapse maturation and plasticity. *Neuron* 54: 583–597.
- Ozaki M, Sasner M, Yano R, Lu HS, Buonanno A (1997) Neuregulin-beta induces expression of an NMDA-receptor subunit. *Nature* 390: 691–694.
- Kato T, Abe Y, Sotoyama H, Kakita A, Kominami R, et al. (2010) Transient exposure of neonatal mice to neuregulin-1 results in hyperdopaminergic states in adulthood: implication in neurodevelopmental hypothesis for schizophrenia. *Mol Psychiatry* doi: 10.1038/mp.2010.10.
- Neddens J, Buonanno A (2010) Selective populations of hippocampal interneurons express ErbB4 and their number and distribution is altered in ErbB4 knockout mice. *Hippocampus* 20: 724–744.
- Dickerson JW, Hemmerle AM, Numan S, Lundgren KH, Seroogy KB (2009) Decreased expression of ErbB4 and tyrosine hydroxylase mRNA and protein in the ventral midbrain of aged rats. *Neuroscience* 163: 482–489.
- Zhang L, Fletcher-Turner A, Marchionni MA, Apparsundaram S, Lundgren KH, et al. (2004) Neurotrophic and neuroprotective effects of the neuregulin glial growth factor-2 on dopaminergic neurons in rat primary midbrain cultures. *J Neurochem* 91: 1358–1368.
- Arguello PA, Gogos JA (2006) Modeling madness in mice: one piece at a time. *Neuron* 52: 179–196.
- Sams-Dodd F (1995) Distinct effects of d-amphetamine and phencyclidine on the social behaviour of rats. *Behav Pharmacol* 6: 55–65.
- Sams-Dodd F (1996) Phencyclidine-induced stereotyped behaviour and social isolation in rats: a possible animal model of schizophrenia. *Behav Pharmacol* 7: 3–23.
- Clemens KJ, Van Nieuwenhuyzen PS, Li KM, Cornish JL, Hunt GE, et al. (2004) MDMA ("ecstasy"), methamphetamine and their combination: long-term changes in social interaction and neurochemistry in the rat. *Psychopharmacology (Berl)* 173: 318–325.
- Rossato JI, Bevilacqua LR, Izquierdo I, Medina JH, Cammarota M (2009) Dopamine controls persistence of long-term memory storage. *Science* 325: 1017–1020.
- Prevot V, Rio C, Cho GJ, Lomniczi A, Heger S, et al. (2003) Normal female sexual development requires neuregulin-erbB receptor signaling in hypothalamic astrocytes. *J Neurosci* 23: 230–239.
- Golub MS, Germann SL, Lloyd KC (2004) Behavioral characteristics of a nervous system-specific erbB4 knock-out mouse. *Behav Brain Res* 153: 159–170.
- Deakin IH, Law AJ, Oliver PL, Schwab MH, Nave KA, et al. (2009) Behavioural characterization of neuregulin 1 type I overexpressing transgenic mice. *Neuroreport* 20: 1523–1528.
- Krivoshaya D, Tapia L, Levinson JN, Huang K, Kang Y, et al. (2008) ErbB4-neuregulin signaling modulates synapse development and dendritic arborization through distinct mechanisms. *J Biol Chem* 283: 32944–32956.
- López-Bendito G, Cautinat A, Sánchez JA, Bielle F, Flames N, et al. (2006) Tangential Neuronal Migration Controls Axon Guidance: A Role for Neuregulin-1 in Thalamocortical Axon Navigation. *Cell* 125: 127–142.
- Roy K, Murtie JC, El-Khodori BF, Edgar N, Sardi SP, et al. (2007) Loss of erbB signaling in oligodendrocytes alters myelin and dopaminergic function, a potential mechanism for neuropsychiatric disorders. *Proc Natl Acad Sci U S A* 104: 8131–8136.
- Davis KL, Stewart DG, Friedman JI, Buchsbaum M, Harvey PD, et al. (2003) White matter changes in schizophrenia: evidence for myelin-related dysfunction. *Arch Gen Psychiatry* 60: 443–456.
- Eyles DW, McGrath JJ, Reynolds GP (2002) Neuronal calcium-binding proteins and schizophrenia. *Schizophr Res* 57: 27–34.
- Akbarian S, Huang HS (2006) Molecular and cellular mechanisms of altered GAD1/GAD67 expression in schizophrenia and related disorders. *Brain Res Rev* 52: 293–304.
- Abe Y, Namba H, Zheng Y, Nawa H (2009) In situ hybridization reveals developmental regulation of ErbB1-4 mRNA expression in mouse midbrain: implication of ErbB receptors for dopaminergic neurons. *Neuroscience* 161: 95–110.
- Yurek DM, Zhang L, Fletcher-Turner A, Seroogy KB (2004) Supranigral injection of neuregulin1-beta induces striatal dopamine overflow. *Brain Res* 1028: 116–119.
- Zheng Y, Watakabe A, Takada M, Kakita A, Namba H, et al. (2009) Expression of ErbB4 in substantia nigra dopamine neurons of monkeys and humans. *Prog Neuropsychopharmacol Biol Psychiatry* 33: 701–706.
- Fumagalli F, Gainetdinov RR, Valenzano KJ, Caron MG (1998) Role of dopamine transporter in methamphetamine-induced neurotoxicity: evidence from mice lacking the transporter. *J Neurosci* 18: 4861–4869.
- Volkow ND, Chang L, Wang GJ, Fowler JS, Franceschi D, et al. (2001) Loss of dopamine transporters in methamphetamine abusers recovers with protracted abstinence. *J Neurosci* 21: 9414–9418.
- Ozaki M, Tohyama K, Kishida H, Buonanno A, Yano R, et al. (2000) Roles of neuregulin in synaptogenesis between mossy fibers and cerebellar granule cells. *J Neurosci Res* 59: 612–623.
- Meuer S, Wittwer C, Nakagawara K (2001) Rapid Cycle Real-Time PCR: Methods and Applications. Heidelberg: Springer Press. pp 21–34.
- Rogers DC, Fisher EM, Brown SD, Peters J, Hunter AJ, et al. (1997) Behavioral and functional analysis of mouse phenotype: SHIRPA, a proposed protocol for comprehensive phenotype assessment. *Mamm Genome* 8: 711–713.
- Karl T, Pabst R, von Hörsten S (2003) Behavioral phenotyping of mice in pharmacological and toxicological research. *Exp Toxicol Pathol* 55: 69–83.
- Kasai A, Shintani N (2007) First screening for behavioral phenotype of gene-engineered mice. *Nippon Yakurigaku Zasshi* 130: 281–285.

55. Frankland PW, Josselyn SA, Anagnostaras SG, Kogan JH, Takahashi E, et al. (2004) Consolidation of CS and US representations in associative fear conditioning. *Hippocampus* 14: 557–569.
56. Mohn AR, Gainetdinov RR, Caron MG, Koller BH (1999) Mice with reduced NMDA receptor expression display behaviors related to schizophrenia. *Cell* 98: 427–436.
57. Mizuno M, Sotoyama H, Narita E, Kawamura H, Namba H, et al. (2007) A cyclooxygenase-2 inhibitor ameliorates behavioral impairments induced by striatal administration of epidermal growth factor. *J Neurosci* 27: 10116–10127.

Full Paper

Antipsychotic Potential of Quinazoline ErbB1 Inhibitors in a Schizophrenia Model Established With Neonatal Hippocampal Lesioning

Makoto Mizuno¹, Yuriko Iwakura², Masako Shibuya², Yingjun Zheng², Takeyoshi Eda², Taisuke Kato², Yohei Takasu², and Hiroyuki Nawa^{1,2,*}

¹Center for Transdisciplinary Research, ²Molecular Neurobiology, Brain Research Institute, Niigata University, Niigata 951-8585, Japan

Received April 8, 2010; Accepted September 9, 2010

Abstract. Hyper-signaling of the epidermal growth factor receptor family (ErbB) is implicated in the pathophysiology of schizophrenia. Various quinazoline inhibitors targeting ErbB1 or ErbB2–4 have been developed as anti-cancer agents and might be useful for antipsychotic treatment. In the present study, we used an animal model of schizophrenia established by neonatal hippocampal lesioning and evaluated the neurobehavioral consequences of ErbB1-inhibitor treatment. Subchronic administration of the ErbB1 inhibitor ZD1839 to the cerebroventricle of rats receiving neonatal hippocampal lesioning ameliorated deficits in prepulse inhibition as well as those in the latent inhibition of tone-dependent fear learning. There were no apparent adverse effects on basal learning scores or locomotor activity, however. The administration of other ErbB1 inhibitors, PD153035 and OSI-774, similarly attenuated the prepulse inhibition impairment of this animal model. In parallel, there were decreases in ErbB1 phosphorylation in animals treated with ErbB1 inhibitors. These results indicate an antipsychotic potential of quinazoline ErbB1 inhibitors. ErbB receptor tyrosine kinases may be novel therapeutic targets for schizophrenia or its related psychotic symptoms.

Keywords: antipsychotic, hippocampal lesion, schizophrenia, epidermal growth factor (EGF), epidermal growth factor receptor (EGFR)

Introduction

Cytokines and growth factors strongly influence neuronal phenotypic differentiation and subsequent brain functions. Previous research suggests that abnormalities in cytokine/growth factor signaling have been implicated in the etiology or neuropathology of schizophrenia (1–4). Previously, we reported the upregulation of epidermal growth factor (EGF) receptor (ErbB1) in forebrain regions of postmortem brains of schizophrenia patients (5). Deficits in EGF signals have also been documented in the peripheral blood of patients (5, 6). In addition, ErbB1 forms heteromeric receptor complexes with neuregulin-1 receptor (ErbB3 and ErbB4) and influences

neuregulin-1 signaling as well (7–9). These findings indicate that impaired EGF/ErbB1 signals might be associated with acute and/or chronic phases of schizophrenia. In agreement with the postmortem results, intrastriatal infusion of EGF to adult rats as well as neonatal administration of ErbB1 ligands perturbs dopaminergic development or function and induces schizophrenia-related abnormalities in cognitive and behavioral traits, although the molecular mechanism of the hyper ErbB1 signals leading to the deficits is not fully resolved (10–14). Recently, we found that the EGF-induced behavioral deficits can be ameliorated by treatment with emodin, a broad tyrosine kinase inhibitor (15). These findings suggest that pharmacological blockade of ErbB1 receptors may be beneficial in the treatment of schizophrenia-associated behavioral deficits.

Based upon the neurodevelopmental hypothesis of schizophrenia, a neonatal ventral hippocampal lesion

*Corresponding author. hnawa@bri.niigata-u.ac.jp
Published online in J-STAGE on October 14, 2010 (in advance)
doi: 10.1254/jphs.10099FP

(VHL) model for schizophrenia was established in rats and has extensively been used to explore the molecular and pharmacological mechanisms underlying the behavioral abnormalities associated with schizophrenia (16, 17). The behavioral abnormalities include hyperresponsiveness to stress (18); decreased social interactions (19); hypersensitivity to MK-801, apomorphine, and amphetamine (20, 21); and impaired prepulse inhibition (PPI), latent inhibition, and working memory (22–25), some of which can be ameliorated by treatment with antipsychotics (19, 20, 26, 27). The VHL model shares not only these behavioral aspects with schizophrenia but also the neurochemical and pharmacological endophenotypes (28–31). Therefore, this model appears to be one of the best animal models to represent the behavioral, pharmacological, and molecular pathological features of schizophrenia and is, therefore, often used for pharmacological evaluation of antipsychotic agents.

Employing this animal model, we assessed the antipsychotic effects of ErbB1 inhibitors. Specifically, we studied the pharmacological actions of the quinazoline derivatives targeting ErbB1, which were developed and are prescribed for anti-cancer therapy (32, 33). We also discuss the potential of ErbB1 inhibitors as novel antipsychotics.

Materials and Methods

Subjects

Male Sprague-Dawley rats (postnatal day 2) were purchased with dams from SLC (Hamamatsu, Shizuoka). Litters were designed born on postnatal day 1 and culled to 10 male pups with their dam by the venter. Rats (8–10 pups plus their dam or 3–4 rats after weaning) were housed in a polypropylene cage (58 cm L × 28 cm W × 24 cm H) and given free access to food and water. The cages were kept in a temperature-controlled colony room (22.0 ± 1.0°C) and maintained under a 12-h light-dark cycle (7:00 on – 19:00 off). We used five independent cohorts of neonatal rats with VHL or sham operations (total n = 143). All of the animal experiments described here were approved by the Animal Use and Care Committee of Niigata University and performed in accordance with the Guiding Principles for the Care and Use of Laboratory Animals (National Institutes of Health, Bethesda, MD, USA). All efforts were made to minimize both the suffering and number of animals used in this study.

Ventral hippocampal lesioning

When the male rat pups reached a body weight of 15–18 g (approximately postnatal day 7–8), they were randomly assigned to receive either sham or lesion status

within each litter. The pups were anesthetized by hypothermia (18); that is, they were placed in wet ice until they did not respond to tail pinch. The rat pup was then immediately immobilized on a platform fixed to a stereotaxic instrument (Narishige Corp., Tokyo) with surgical tapes, and a 10-mm incision was made in the skin overlying the skull. Ibotenic acid solution (0.3 μL, 3 μg; Sigma-Aldrich, St. Louis, MO, USA) or an equal volume of phosphate-buffered saline was injected to the ventral hippocampus in each hemisphere over a period of 2 min through a 30-gauge cannula positioned at the following coordinates: 3.2-mm posterior, ±3.5-mm lateral to the bregma, and 5.0-mm below the dura. The cannula remained in place for another 3 min to complete the infusion, and the skin incision was closed with two stitches. The pups were warmed with a heat pad and then returned to their mothers. On postnatal day 20–23, the pups were weaned, separated by lesion status, and grouped two or three to a cage.

Intracerebroventricular infusion of ErbB1 inhibitors

The procedure for drug infusion into the rat brain has been described previously (34). After confirming deep anesthesia with sodium pentobarbital (50 mg/kg, i.p.; Dainippon-Sumitomo Pharmaceutical Co., Ltd., Osaka), we secured each rat (postnatal day 54–60) to a stereotaxic apparatus (Narishige Corp.) with the upper incisor bar set 3.0-mm below the interaural line. We exposed the skull, drilled a hole, and implanted a 30-gauge cannula (Terumo, Tokyo), which was implanted in the right side of the lateral ventricle (0.3-mm posterior and 1.2-mm right lateral measured from the bregma, 4.5-mm below the dura), glued to the skull, and connected to an Alzet osmotic minipump (model 2002, a two week type; Alza Corp., Palo Alto, CA, USA) by medical grade vinyl tubing. The minipump was filled with a 10% DMSO solution containing PD153035 (1.0 mg/mL), ZD1839 (1.0 mg/mL), OSI-774 (0.1 mg/mL), or 10% DMSO alone (vehicle) and implanted subcutaneously into the nape of the neck. The solution was administered continuously at a rate of 0.5 μL/h from the minipump. The scalp incision was closed with surgical staples and treated with Cefmetazon, a topical antiseptic (50 mg/day; Sankyo Pharmaceuticals, Inc., Tokyo). We confirmed the position of the cannula after completion of the behavioral tests. The ErbB1 inhibitors, PD153035 [4-(3-bromophenylamine)-6,7-dimethoxy-quinazoline; Calbiochem, San Diego, CA, USA], ZD1839 [gefitinib, 4-(3-chloro-4-fluorophenylamine)-7-methoxy-6(3-(4-morpholinyl)-quinazoline; AstraZeneca Pharmaceuticals, Osaka], and OSI-774 (erlotinib, 4-(3-ethynylphenylamine)-6,7-bis(2-methoxyethoxy)-quinazoline; OSI Pharmaceuticals, Melville, NY, USA) were dissolved in 100% DMSO,

diluted with saline, and added to an osmotic minipump (35). The effective doses were determined in another animal model for schizophrenia (M. Mizuno, unpublished data).

Schedule of behavioral testing, drug treatment, and dissection

After a recovery period of at least five days following minipump implantation, rats were subjected to behavioral testing. However, this testing had to be completed before the minipump was depleted of drug (i.e., 14 days after surgery). To avoid interactions between independent behavioral tests, rats were given more than two days of recovery between the behavioral tests. The rats also received the behavioral tests in order of increasing stress to the animal: locomotor activity test, acoustic startle test, and contextual conditioning. Fifty two rats receiving VHL were sacrificed after the completion of behavioral testing to confirm the position of the hippocampal lesions and cannula placement. The other VHL rats were sacrificed in order to measure ErbB1 phosphorylation in brain tissues.

Histochemistry

Rats receiving VHL or drug infusions were transcardially perfused with 4% paraformaldehyde in a 0.1 M phosphate-buffered solution (pH 7.4). After post-fixation, brains were immersed in 15% and 30% sucrose solutions and frozen in O.C.T. Compound (Tissue-Tek, Miles, Inc., Elkhart, IN, USA). Coronal sections (15- μ m-thick) were cut from frozen brains and stained with a 0.1% cresyl violet solution.

Western blotting

To verify the action of ErbB1 inhibitors, we measured phosphorylated and total levels of ErbB1 protein in rats receiving PD153035, ZD1839, or vehicle by Western blotting. Rats were anesthetized with halothane and brains were dissected immediately after decapitation. Brains were immersed in ice-cold phosphate-buffered saline and sliced. Frontal cortex, striatum and the region surrounding the lateral cerebroventricle were dissected and homogenized by sonication in 2% sodium dodecyl sulfate (SDS) buffer containing phosphatase inhibitors (2 mM NaVO₄ and 10 mM NaF) and a protease inhibitor cocktail (Complete Mini; Roche, Mannheim, Germany). Tissue lysates were centrifuged at 13,000 rpm for 10 min at 4°C, and the supernatants were stored at -80°C until further use. Protein samples (50 μ g/lane) were denatured with 8% β -mercaptoethanol plus 2% SDS, separated by SDS-polyacrylamide gel electrophoresis, and transferred to a PVDF membrane (Immobilon; Millipore, Billerica, MA, USA). The membrane was probed with the anti-

phospho-ErbB1 antibody (1:1000; Cell Signaling Technology, Danvers, MA, USA), anti-ErbB1 antibody (1:1000, Cell Signaling Technology), and anti- β -actin antibody (1:2000, Millipore). After extensive washing, immunoreactivity on the membrane was detected with the anti-rabbit immunoglobulin antibody conjugated to horseradish peroxidase (Jackson Immunoresearch Laboratory, West Grove, PA, USA) followed by a chemiluminescence reaction (ECL kit; Perkin Elmer, Yokohama). Densitometric quantification of band intensity was performed with Image J (National Institutes of Health).

Measurement of acoustic startle and PPI

We measured acoustic startle and PPI responses of rats receiving PD153035, OSI-774, ZD1839, or vehicle in a startle chamber (SR-Lab Systems; San Diego Instruments, San Diego, CA, USA) adapted for rats (36–38). The chosen paradigm was used to assess the startle amplitude, habituation, and PPI response with acoustic stimuli of 120 dB, a single prepulse interval (100 ms), and three different prepulse intensities [5, 10, and 15 dB above background noise (white noise, 70 dB)]. To acclimatize the rat to the startle chamber, each rat was placed in the chamber for 5 min with background noise alone. The rat was then subjected to 50 startle trials; each trial consisting of one of five conditions: i) a 40-ms 120-dB startle tone presented alone (S); ii–iv) a 40-ms 120-dB startle tone following prepulses by 100 ms (20-ms duration) that were 5, 10, or 15 dB above background noise (i.e., 75-, 80-, or 85-dB prepulse, respectively); or v) no stimulus (N, background noise alone), which was used to measure baseline movement in the chamber. In the PPI test, these five trial types (i–v) were repeated eight times each in a pseudorandom order for a total of 40 trials. Each trial type was presented once within a block of five trials. At the beginning and end of the PPI test, five consecutive trials of (i) were presented to assess habituation during the sessions. The inter-trial interval of the PPI tests was 15 s. The analysis of the PPI responses was based on the mean of the eight trials for each trial type. The percentage PPI of a startle response was calculated as: $100 - [(startle\ response\ on\ prepulse - pulse\ stimulus\ trials - no\ stimulus\ trials) / (pulse-alone\ trials - no\ stimulus\ trials)] \times 100$.

Locomotor activity

We measured rat locomotor activity in a novel environment, consisting of a large behavioral chamber, using a procedure described previously (10). The rat receiving ZD1839 or vehicle was placed in an open field box (45 cm L \times 45 cm W \times 30 cm H; MED Associates, St. Albans, VA, USA) under moderate light level (400 lx). Line crossings and rearing counts were measured by